

# Thesis Report

## Siddharth Narayanan

Modelling and performance analysis of an integrated control system for providing ancillary services using a BESS





# Thesis Report

by

Siddharth Narayanan

to obtain the degree of Master of Science  
at the Delft University of Technology,  
to be defended publicly on Monday May 27, 2019 at 03:00 PM.

Student number: 4720369  
Project duration: Sep 1, 2018 – May 27, 2019  
Thesis committee: Prof. dr. P. Palensky, TU Delft  
Dr. M. Cetkovic, TU Delft, supervisor  
Dr. T. B. Soeiro, TU Delft, External supervisor

An electronic version of this thesis is available at <http://repository.tudelft.nl/>.



# Preface

I am grateful to my family and friends for their constant support and encouragement throughout the course of my thesis. I am honoured to have the guidance of Prof. Peter Palensky, Asst. Prof. Milos Cvetkovic and Umer Mustaq during my thesis project and I am also thankful for the opportunity to learn and to contribute to ongoing research. Next, I would like to thank Asst. Prof. Thiago Batista Soeiro for agreeing to be part of my thesis committee, and taking the time to evaluate my work.

Furthermore, I would like to appreciate the timely support of Ellen with administrative tasks. Finally, I would like to appreciate the prompt and helpful support of the RTDS support team. This work is performed in collaboration with EASYRES project of European Union Horizon 2020 initiative with Grant agreement: 764090.

*Siddharth Narayanan*  
*Delft, May 2019*



# Abstract

The production and consumption of energy in all walks of life is moving towards a greener and more sustainable mix of energy sources away from the traditional sources of coal and gas. With this shift, more renewable energy is expected to be integrated into the grid replacing conventional synchronous generators. In such conditions, the stability of the grid becomes a major concern due to the lack of inertia with the loss of base load generators. As a result, there is an urgent need to develop flexible solutions like Battery Energy Storage System (BESS) to provide ancillary services. Current research tackles it with a piecemeal approach towards frequency and voltage stability. As a result, different types of controller topology are currently used to get each electrical parameter within the acceptable tolerance limits.

The contribution of this thesis is to build an integrated controller based on droop control to tackle the two parameters of voltage and frequency stability simultaneously with one controller in a holistic fashion. To achieve this goal of demonstrating integrated control, different control schemes were tested and compared in terms of performance with respect to frequency control. The application of the above mentioned integrated control in a decentralized controller environment like a virtual power plant (VPP) was also demonstrated. The testing and design of the control schemes and BESS was done via benchmark models built for real time digital simulation (RTDS). The results show that the control schemes employed in the BESS can effectively contribute towards providing ancillary services in a holistic manner.



# Contents

<b>List of Tables</b>	<b>ix</b>
<b>List of Figures</b>	<b>xi</b>
<b>1 Introduction</b>	<b>1</b>
1.1 Motivation . . . . .	2
1.2 Problem definition . . . . .	3
1.3 Objective . . . . .	3
1.4 Research Questions . . . . .	3
1.5 Methodology . . . . .	3
1.6 Thesis Contribution . . . . .	3
1.7 Thesis Outline . . . . .	4
<b>2 Background</b>	<b>5</b>
2.1 Grid services . . . . .	5
2.2 Control methodology . . . . .	6
2.3 Virtual Power Plant . . . . .	7
2.4 BESS coordination . . . . .	7
2.5 Time Delay in power systems . . . . .	8
2.6 Voltage Source Converter (VSC) . . . . .	8
2.6.1 Model . . . . .	8
2.6.2 Transformation steps . . . . .	8
2.6.3 Control Loops . . . . .	12
<b>3 Methodology and Implementation in RTDS</b>	<b>17</b>
3.1 CIGRE Model . . . . .	17
3.1.1 Background . . . . .	17
3.1.2 Medium Voltage Network Benchmark . . . . .	18
3.1.3 Topology of MV benchmark network . . . . .	19
3.2 Underground cables . . . . .	21
3.3 Generator model . . . . .	22
3.4 Battery model . . . . .	22
3.5 PV source model . . . . .	24
3.6 BESS Control Schemes . . . . .	24
3.6.1 Primary Frequency Control . . . . .	24
3.6.2 Peak Shaving . . . . .	25
3.6.3 Integrated control . . . . .	25
3.6.4 Integrated control with multiple BESS . . . . .	25
3.6.5 Integrated control with time delay . . . . .	26
3.6.6 Micro-grid voltage control . . . . .	26
<b>4 Results &amp; Discussions</b>	<b>27</b>
4.1 Network Scenarios . . . . .	27
4.2 Applications . . . . .	27
4.3 Primary Frequency control (Traditional Control Scheme) . . . . .	28
4.4 Peak Shaving (PS) services & Primary Frequency control . . . . .	29
4.5 Integrated control for Primary Frequency control . . . . .	30
4.6 Integrated control for Primary Frequency & Voltage Control . . . . .	31
4.7 Primary Frequency Control with Two BESSs . . . . .	32
4.8 Primary Frequency Control with Three BESSs . . . . .	33
4.9 Primary Frequency Control with Time Delay . . . . .	35

4.10 Voltage control in Micro-grid mode . . . . .	37
4.11 Controller Tuning . . . . .	39
4.11.1 Voltage control . . . . .	39
4.11.2 Primary frequency control and Steady state contribution. . . . .	41
<b>5 Conclusions and Recommendations</b>	<b>45</b>
5.1 Summary of Observations and Key Insights . . . . .	45
5.2 Conclusions. . . . .	46
5.3 Contributions to IEPG . . . . .	47
5.4 Future work . . . . .	47
<b>A User Manual</b>	<b>49</b>
A.1 Objective . . . . .	49
A.2 Procedure. . . . .	49
A.2.1 LOADING THE DRAFT FILE . . . . .	49
A.2.2 Power calculation block . . . . .	49
A.2.3 Runtime. . . . .	49
<b>B RTDS: Hardware and Software Introduction</b>	<b>53</b>
B.1 RTDS Hardware . . . . .	54
B.2 RTDS Software Interface. . . . .	56
B.3 Software Implementation in RTDS. . . . .	60
<b>C RSCAD control schemes</b>	<b>61</b>
C.0.1 BESS Control Block . . . . .	61
C.0.2 PV Control Block . . . . .	62
C.0.3 Primary Frequency Control . . . . .	62
C.0.4 Frequency & Peak Shaving Control . . . . .	63
C.0.5 Integrated Control . . . . .	64
C.0.6 Integrated Control with Multiple BESS . . . . .	65
C.0.7 Integrated Control with Time delay . . . . .	66
C.0.8 Microgrid Voltage control. . . . .	67
<b>Bibliography</b>	<b>69</b>

# List of Tables

3.1 Connections and line parameters of European MV distribution network benchmark Line [52] . . . . . 20



# List of Figures

1.1	Net generation by plant type in EU28 in the EUCO30 scenario [3]	1
2.1	Control strategy architectures [34]	6
2.2	Overview of different aspects of the VSC model [48]	9
2.3	Single Line Diagram of VSC [48]	10
2.4	Simple circuit of a phase reactor [48]	10
2.5	Phasors in the abc frame for $t=t_1$ and $t=t_2$ [48]	11
2.6	Phasors in the $\alpha\beta$ frame for $t=t_1$ and $t=t_2$ [48]	11
2.7	Phasors in the dq frame for $t=t_1$ and $t=t_2$ [48]	11
2.8	The steps of the transformation [48]	12
2.9	Diagram of the control architecture [48]	12
2.10	Control Block of the PLL [48]	13
2.11	Operation of PLL[48]	13
2.12	The open Loop VSC [48]	14
2.13	The closed loop VSC [48]	14
2.14	Overview of the control loops of the VSC [48]	15
3.1	Hierarchy for identifying benchmarks [52]	17
3.2	Topology of European MV distribution network benchmark 6.2.2 [52]	19
3.3	Benchmark network on RSCAD	20
3.4	Single and Three Phase Average Models for DC sources	21
3.5	PI section model in RSCAD	21
3.6	Generator model in RSCAD	22
3.7	Battery model in RSCAD	22
3.8	Battery control representation	23
3.9	PV source model	24
3.10	V/F Droop Control	24
3.11	Primary Frequency control	25
3.12	Primary Frequency control & Peak Shaving	25
3.13	Integrated control	25
3.14	Integrated control with multiple BESS	26
3.15	Integrated control with time delay	26
4.1	Primary Frequency Control with and without BESS - Step Load	28
4.2	Peak shaving contribution	29
4.3	Different control schemes	30
4.4	Integrated control for Primary frequency control & Voltage Control	31
4.5	Integrated control with multiple BESS	32
4.6	Frequency comparison for coordination of multiple BESS	33
4.7	Comparison of frequency for different measurement techniques	34
4.8	Comparison of frequency for different BESS power limits	34
4.9	Integrated control with time delay	35
4.10	Micro-grid - Island mode	36
4.11	Micro-grid - Island mode (Step disturbance)	36
4.12	Micro-grid - Grid Transition	37
4.13	Grid connected voltage control with and without BESS - Step Load	38
4.14	Grid connected voltage control Sensitivity Analysis for $K_p$ - Step Load	39
4.15	Grid connected voltage control Sensitivity Analysis for $K_i$ - Step Load	40
4.16	Sensitivity analysis for $K_p$	41

4.17 Primary Frequency Control Sensitivity Analysis for $K_i$ - Step Load . . . . .	42
4.18 Primary Frequency Control Sensitivity Analysis for Droop - Step Load . . . . .	42
A.1 Benchmark network on RSCAD . . . . .	50
A.2 Benchmark network on RSCAD . . . . .	50
A.3 Benchmark network on RSCAD . . . . .	51
B.1 A typical RTDS hardware setup . . . . .	53
B.2 RTDS GTWIF card . . . . .	54
B.3 The RTDS Global Bus Hub . . . . .	54
B.4 The RTDS PB5 processor card . . . . .	55
B.5 The RTDS NOVACOR . . . . .	55
B.6 RTDS File Manager Module . . . . .	56
B.7 RTDS Draft Module . . . . .	57
B.8 RTDS Power System and Control Library . . . . .	57
B.9 RTDS RunTime module . . . . .	58
B.10 RTDS TLine module . . . . .	58
B.11 RTDS Cable module . . . . .	59
B.12 RTDS Cbuilder module . . . . .	59
C.1 BESS control block . . . . .	61
C.2 PV control block . . . . .	62
C.3 Frequency control . . . . .	62
C.4 Frequency & Peak-shaving control . . . . .	63
C.5 Integrated control . . . . .	64
C.6 Integrated control with multiple BESS . . . . .	65
C.7 Integrated control with time delay . . . . .	66
C.8 Micro-grid voltage control . . . . .	67
C.9 Voltage control during transition . . . . .	67

## Introduction

The production of electricity is moving towards a greener and more sustainable mix of energy sources away from the traditional sources of coal and gas. This is due to an initiative to facilitate the shift towards renewable sources of energy after the international agreement at the Conference of the Parties (COP21) to cap the global temperature rise to 2 degrees Celsius [1]. As a result, the penetration of renewable energy in the grid has been steadily increasing, especially in developed countries. This trend is expected to accelerate in the coming decades and expected to pose significant technical challenges.

Renewable energy production is expected to account for 85% of the total global electricity production by 2050. Moreover, transportation and heat pump sectors are undergoing a transition to electricity leading to higher demands on existing transmission and distribution networks [2]. The projected energy mix for the year 2050 is as shown in Figure 1.1 [3]. The stability of the electrical grid becomes a concern with increased penetration of renewable energy based technologies coupled with the loss of synchronous generators powered by fossil fuels.

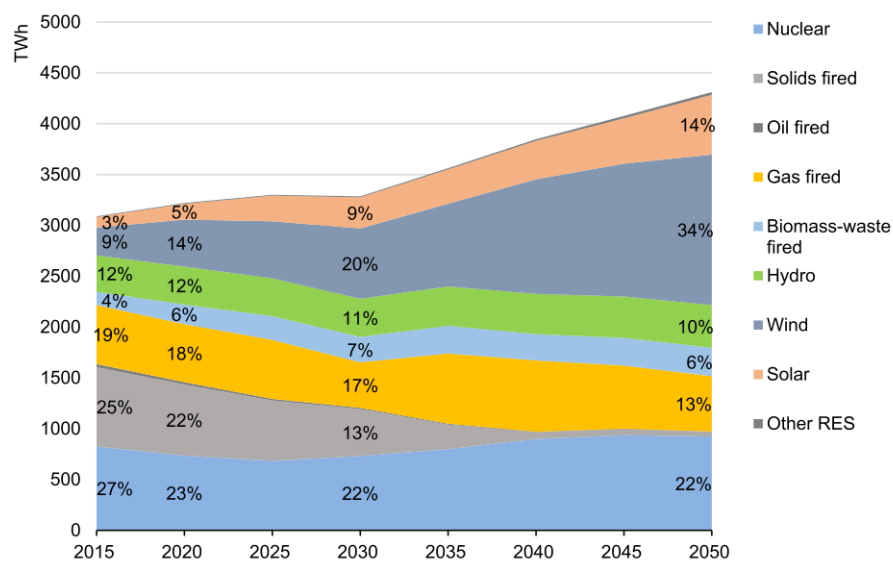


Figure 1.1: Net generation by plant type in EU28 in the EUCO30 scenario [3]

## 1.1. Motivation

The transition to renewable energy has led to an urgent need to research and develop innovative flexible solutions to maintain the stability of the network [4]. These solutions have come to be known as ancillary services. Conventionally, the flexibility of the electrical grid comes from synchronous generators which help maintain the voltage and frequency around their nominal values. With phased decommissioning of the synchronous generators, ancillary services become essential for the successful integration of intermittent sources of energy like solar and wind. The absence of such services will lead to greater volatility and problems in stability and reliability and customers can experience lower quality of power supply or even outage which is undesirable.

There are different types of technologies currently available in the market for implementing ancillary services including batteries energy storage systems (BESS), capacitors, pumped hydroelectric storage, compressed air storage, flywheel storage, superconducting magnetic energy storage, and thermal energy storage. With the advancement of power electronics and battery technology, BESS is also becoming more economically viable to compete with the other solutions as the price of batteries fall due to economies of scale. It also provides alternatives to conventional storage like pumped hydro since it can store off peak energy and discharge during peak times. Moreover, BESS is ideal for providing ancillary services due to its fast response time and high ramp rates. This helps defer and possibly eliminate the capital investment necessary for transmission or distribution lines and also helps reduce the stress on existing generation sources. In addition to providing grid connected services, BESS can also help off grid setups by facilitating black start services [5][6].

Coordination of BESSs becomes vitally important with the increasing use of DER. The capacity of each DER is not enough to provide ancillary services on its own but they can be aggregated to participate in the market. Coordination becomes important when it comes to dealing with multiple BESSs due to risk of regulation failure when some BESSs exhaust their energy capacity before others. This thesis explores and demonstrates the possibility of using the integrated control algorithm to engage and coordinate multiple DERs to provide frequency support services without the need for a centralized control system [7].

As mentioned earlier, a lot of research has gone into tackling the electrical parameters such as voltage [8][9][10] and frequency control separately [11][12][13]. Solutions for voltage control in distribution network are still in pilot stages and not standardized yet. Peak shaving also becomes important with increasing variability in generation. This was traditionally taken care by spinning reserves powered by fossil fuels [14]. Conventionally, for droop control in AC networks with high reactive impedance, active power depends on the bus angles and the reactive power depends on the magnitude of the voltage. This leads to the classical  $f$ - $P$  and  $V$ - $Q$  droop control algorithm. The use of VSC in droop control for providing ancillary services employs the concept of vector current control ( $dq$ ) to achieve the required voltage and frequency values. Delays in communication and sensing can also play an equally important role in the controller design and needs to be thoroughly investigated. [15][16].

Current research tackles the above-mentioned challenges with a piecemeal approach towards frequency and voltage stability [17]. As a result, different types of controller topology are currently used to get the electrical parameters within the acceptable tolerance limits of their nominal values [18]. With the number of ancillary services provided by single power source like BESS increasing, the number of controllers would exponentially increase when more distributed energy resources (DERs) start taking part in the market. To tackle this, it is important to explore and develop integrated controllers to provide two or more ancillary services with the same controller. The contribution of this thesis is to build an integrated controller based on droop control to tackle the two parameters of voltage and frequency stability simultaneously with one controller in a holistic fashion. This is different from the current trend of ancillary services which aims to control frequency and voltage separately as explained above. Droop control was chosen over other forms of control to build the inte-

grated control due to its simplicity of application. Using strategies based on communication increase the complexity and reduce the reliability and expandability of the system by basing it on the communication links. Moreover, the droop control method is very suitable for modular design which improves the flexibility and redundancy of the system. This helps in maintaining a reliable and stable system which is easy to expand and use for industry applications.[19][20][21].

## 1.2. Problem definition

It can be seen that there is a lack of research done in developing an integrated controller to tackle many of the the power quality issues at the same time in a holistic fashion. The contribution of this thesis will be to bridge that knowledge gap and develop an integrated controller to provide ancillary services using a BESS.

## 1.3. Objective

To model an integrated control system based on droop control for providing ancillary services using a BESS and to validate it using a standard CIGRE model on RSCAD. The conditions are simulated for different levels of renewable energy penetration to reflect the short, mid and long term nature of renewable energy integrated grids. The simulations are done in RSCAD as it offers a safe and controlled environment to get precise results in a real time simulation setup.

## 1.4. Research Questions

1. What is the effect of the BESS on the overall stability and the performance of generator in the system?
2. How does the BESS perform in the case of black start scenarios?
3. Does the performance of a VPP improve with the implementation of adaptive SOC based droop?
4. Is the performance of an integrated control system better than building individual controls?
5. How robust is the controller when it comes to dealing with time delays in the inverter hardware?
6. How does the controller perform for different levels of renewable energy penetration in the grid?
  - 1) 30 %
  - 2) 50 %
  - 3) 98 %

## 1.5. Methodology

The system and the controller was developed and tested using mathematical modelling and real time simulation. It was carried out in a simulation setup created on RSCAD and processed using the RTDS hardware. This approach was favoured as it enables the researcher to test the control logic in a cost effective way without compromising the usefulness of the study. Chapter 3 will explain this in more detail.

## 1.6. Thesis Contribution

The contribution of the thesis is as follows:

1. Design and application of novel control algorithms such as peak shaving and integrated controller model and implementation of an adaptive droop controller model for BESS in RSCAD.
2. Robustness study of the BESS controller with respect to time delay.
3. CIGRE model in RSCAD and a comparison study of the performance of the integrated controller with respect to individual controllers

## **1.7. Thesis Outline**

Chapter 1 presents an overview of the situation in the electrical systems and the need for an integrated controller for ancillary services provided by BESS. Chapter 2 explains the control theory concept involved in the integrated controller for BESS. The implementation of the controller is described in Chapter 3. The results are illustrated and discussed in Chapter 4 and Chapter 5 concludes the report and discusses future work.

# 2

## Background

This chapter focuses on the different grid services provided by the BESS and the functionality of the VSC. The first section will describe the common grid services provided by the BESS with the second section going deeper into the inner workings of a VSC in terms of its system architecture and control loops.

### 2.1. Grid services

The impact of BESS on the utility network is increasing and it is crucial as a solution to stability problems. As discussed in Chapter 1, integration of more renewable sources creates a need for balancing sources like BESS due to the intermittent nature of RES causing voltage and frequency fluctuations in the grid network [22][23]. The installation of large storage capacity in the grid network will enable a high penetration of wind and solar in the electricity mix. A case study was conducted in Portugal with the case of a wind farm having an installed capacity of 144-MW. It was seen that the wind farm was generating more off peak energy than in peak hours making the project economically unsustainable. The addition of a 5 MW, 30 MWh BESS was proposed to shift some of the generated power from off peak to peak hours to improve the economic aspects of the wind farm. This resulted in a 2.1% increase in revenue generated from energy tariffs[24][25][26]. The BESS contributes as an ancillary service in many ways with some of its common applications as follows:

- Frequency regulation – Primary control

Modern variable-speed wind turbines and large photo voltaic power plants connected to the utility grid do not contribute to the frequency stability as much as conventional generators. This creates a new application of BESS to emulate the inertia of synchronous generators. Moreover, BESS has the advantage of being capable of responding swiftly and precisely to frequency deviations making it one of the best solutions for primary frequency response.

- Reliability

The presence of a BESS improves the overall reliability of the power system. The reduced time response of the BESS enables it to react immediately after a disturbance. For example, it can help to maintain the stability of the network while the grid operator re-dispatches a generator [27]. It can also improve the local resilience of the system if there is a fault in the transmission network due to natural disasters. BESS can act as a good emergency power supply and help with the black start of a medium voltage network in the event of climate disasters and terrorist attacks [28]. The application of BESS to form a grid in the event of a black start with the subsequent transition to a grid following mode after the generator is brought online is described and illustrated in Chapters 3 & 4.

- Power quality

The quality of power supply is crucial in industrial processes like semiconductor manufacturing. A BESS integrated at the distribution level can ensure that by smoothing voltage variations. As discussed earlier, this holds true for black starts as well. Moreover, RES combined with BESS improves the power quality of the output by absorbing or injecting reactive power thereby keeping the real power constant as per load requirements [29].

- Voltage regulation

It has been seen that integrating BESS in a power system helps to support voltage in distribution networks. The voltage deviation can be reduced by installing a BESS in a distribution network. The penetration levels of PV can be improved with the integration of BESS as it can reduce energy loss and enhance voltage stability. It can also regulate active and reactive power in the bus, improving the voltage profile in a network [30].

- Peak Load Shaving

BESS can provide peak load shaving facilities in a power system to shift the load from peak to off peak periods. However at current prices, BESS is economical only for peak demand periods of less than 1 hr. In a study carried out at the distribution level, it was seen that the peak shaving performance of the BESS was directly influenced by the location and configuration of the installed BESS [31][32][33].

## 2.2. Control methodology

The control methodology employed in power systems is undergoing a radical transformation by moving away from the traditional centralized means of control to distributed and decentralized schemes. This trend is facilitated and driven by the widespread adoption of RES and BESS along with better communication and processing infrastructure

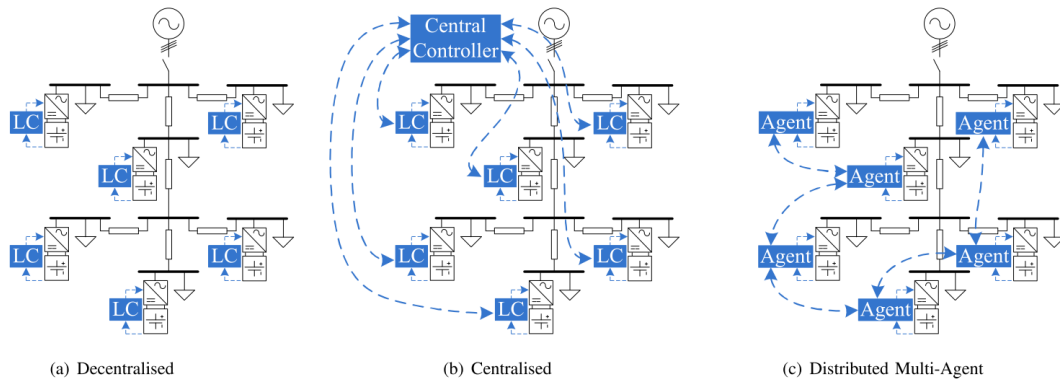


Figure 2.1: Control strategy architectures [34]

The traditional centralized control model does not work well for distributed networks with multiple sources like PV and BESS. The lack of strategies to coordinate such components is a significant factor in moving towards decentralized and distributed mechanisms [34]. The three mechanisms are illustrated in Figure 2.1 and discussed in the following sections.

- Decentralized

The decentralized control strategy is a common method employed to achieve autonomous operation of different components. The standard method is decentralized droop control, which enables load sharing between sources without the need for any communication links. This is similar to the primary level control used in centralized schemes but this is practically possible only in small networks due to the high communication cost involved [35]. Some of the common schemes are listed below:

1. Traditional Droop Control
2. State of Charge weighted Droop Control
3. Droop Control for Heterogeneous Energy Storage Systems

- Centralized

In a centralized control scheme, each component of the system can be individually monitored and controlled. It is the oldest form of control and can be broadly split into two categories, secondary and tertiary control levels. Control schemes with transient objectives such as power quality regulation are considered as secondary while power flow problems based on renewable generation are considered as tertiary. Some of the common schemes are listed below:

1. Centralized Secondary control
2. Centralized AC Micro grid Tertiary control
3. Centralized DC Micro grid Tertiary Control

- Distributed

The decentralized control scheme discussed earlier is a good solution for coordination many sources in a power system but it is not enough to fully harness the combined power and energy capacities of the system. This led to the development of distributed control schemes since the centralized scheme incurs a lot of communication cost along with data privacy concerns. This control scheme involves different components of the system controlled autonomously and is connected by a sparse communication network as shown in Figure 2.1. It is still developing and in the nascent stage of deployment [36][37]. Similar to centralized schemes, control strategies have been proposed for secondary and tertiary levels and are as follows:

1. Distributed Multi-Agent Secondary Control
2. Cooperative Multi-Agent Tertiary Control
3. Competitive Multi-Agent Tertiary Control

## 2.3. Virtual Power Plant

A Virtual Power Plant (VPP) can be considered as a flexible representation of portfolio of different DER sources. It acts as more than just an aggregator of the different DER components by creating a single operating profile from a composite of parameters characterizing each DER similar to that of a traditional transmission connected generator.

A VPP can contain many different types of sources varying from RES like solar and wind to energy storage systems like BESS. It can also contain classical generating units and flexible loads. The presence of units like BESS help the VPP overcome the intermittent nature of RES achieving optimal usage of resources. In recent years, significant developments in ICT have led to increased and efficient deployment of VPP by facilitating decentralized system management. Commercially, VPP has been used in Belgium and Netherlands as a financial instrument in the energy market while Germany and UK allow VPP to offer system balancing and grid ancillary services[38].

## 2.4. BESS coordination

BESS in contrast to other types of DER systems are energy constrained and are therefore limited when it comes to providing regulation service if the state of charge (SOC) limits are hit. As a result, BESS systems need to have strategies to replenish the batteries and recover SOCs to optimal levels during idle time (i.e., when the system frequency is within the nominal range) [39] [40]. Many of the studies are performed for single BESS scenarios providing frequency regulation. In recent years, the number of DER which are BESS have increased with the transition to electric vehicles and home storage devices like Tesla Power wall [41].

Individually, these batteries are not large enough to participate in primary frequency regulation. Therefore, strategies need to be developed to aggregate the capacities of multiple BESSs and provide frequency regulation as a single unit. The challenge for multi BESS systems is the optimal coordination of BESSs during the frequency regulation phase. The coordination needs to be carefully done to ensure that the BESSs don't exhaust their energy capacity before the others, which affects the total energy capacity available and can potentially lead to unnecessary regulation failures [42].

## 2.5. Time Delay in power systems

Time delays are inherently present in physical processes with signal transmission, measurement and control. Studies have been conducted to observe the impact of time delays in power systems [43][44][45]. It was seen that it was necessary to consider the time delays while analyzing the stability of power systems and designing controllers. With the advancement in technology, phasor measurement unit (PMU) devices are widely deployed to control the interconnected power system to improve its dynamic performance. Usually, the latency is limited to milliseconds in modern power systems [46]. However, it can be get higher to the range of hundreds of milliseconds in extreme cases. Moreover, even a small delay could destabilize the power system under certain conditions. With increased distributed generation, it becomes increasingly important to study the impact of time delay in the design of distributed control systems [47].

## 2.6. Voltage Source Converter (VSC)

This section describes the VSC layout and the functionality of a VSC in detail for the reader to understand the inner workings of the converter. A VSC is generally used to convert the DC power generated on one side of the converter (eg: Battery, PV, etc.) into AC power supplied/consumed to/from the grid for different reasons. To enable the VSC to maintain power balance, the voltages on both the AC and DC side are constantly monitored. The monitored values are then adjusted using a feedback loop to ensure the required active and reactive power input into the grid.

### 2.6.1. Model

It is important to understand the layout shown in Figure 2.2[48] to fully appreciate the functionality of VSC. The phase reactor and the grid are important components that influence the power supplied and consumed by the VSC. The single line diagram of the above mentioned VSC is shown in Figure 2.3[49].

**Phase reactor** A simple circuit of the phase reactor can be seen in Figure 2.4[49]. Phase reactors are essentially current limiting devices which are useful in controlling the active and reactive power between the VSC and the grid terminal. This is achieved by controlling the voltage drop across the reactor thereby controlling the angle difference between the two terminals (VSC and grid).

$$u_{c,abc} - u_{s,abc} = r i_{abc} + L \frac{di_{abc}}{dt} \quad (2.1)$$

#### Grid

An infinite grid is assumed for the grid set up which is essentially an ideal voltage source with high impedance.

### 2.6.2. Transformation steps

It is not easy to understand the VSC model using conventional control theory. The most common method of industrial control is PI regulator. However, robust VSC control using PI regulators cannot be achieved through sinusoidal input. To overcome this issue, vector control schemes which employ a rotating dq rotating reference frame were developed. Both

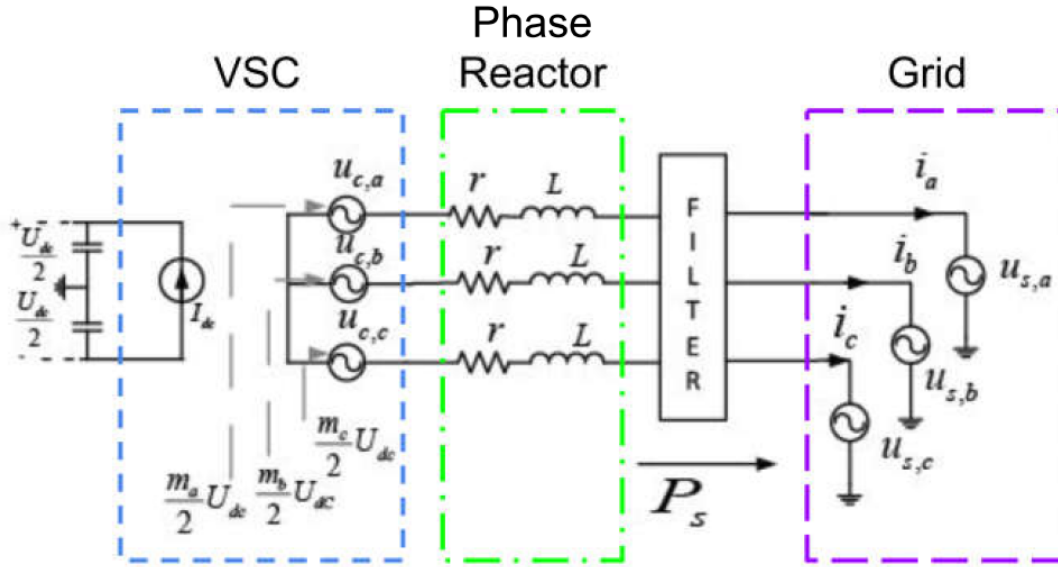


Figure 2.2: Overview of different aspects of the VSC model [48]

AC voltage and current can be transformed into the dq frame from their sinusoidal forms. The conversion is achieved by performing Clark and Park transformation explained below.

#### Clark Transformation

The transformation is better explained with the aid of two Figures 2.5, 2.6 below. Considering Figure 2.5, it can be seen that each phasor represents a phase of a 3 phase sinusoidal value separated by an angle difference of 120 degrees. The sum of the three phases is always the rotating space vector  $v$  even though the magnitude of the individual phasors alternate. The space vector  $v$  would be rotating with a frequency of 50/60 Hz in a conventional grid. The same space vector is plotted on a  $\alpha\beta$  frame in Figure 2.6. On a two dimensional plane, it is enough to have two components to get the same space vector. As a result, it is possible to transform the three phase abc signal into a two-phase  $\alpha\beta$  signal using the Clark transformation. The equations below explain in detail the transformation from abc to  $\alpha\beta$  domain [50].

$$\begin{bmatrix} i_\alpha \\ i_\beta \end{bmatrix} = \frac{2}{3} \begin{bmatrix} 1 & -\frac{1}{2} & -\frac{1}{2} \\ 0 & \sqrt{\frac{3}{2}} & \sqrt{\frac{3}{2}} \end{bmatrix} \begin{bmatrix} i_a \\ i_b \\ i_c \end{bmatrix} \quad (2.2)$$

$$\begin{bmatrix} v_\alpha \\ v_\beta \end{bmatrix} = \frac{2}{3} \begin{bmatrix} 1 & -\frac{1}{2} & -\frac{1}{2} \\ 0 & -\sqrt{\frac{3}{2}} & \sqrt{\frac{3}{2}} \end{bmatrix} \begin{bmatrix} v_a \\ v_b \\ v_c \end{bmatrix} \quad (2.3)$$

$$u_{c,\alpha\beta} - u_{s,\alpha\beta} = r i_{\alpha\beta} + L \frac{d i_{\alpha\beta}}{dt} \quad (2.4)$$

#### Park Transformation

The transformed space vector after the Clark transformation is still sinusoidal and alternates in magnitude during rotation. In order to convert it into a DC signal, each phase must have a constant magnitude. To achieve this, the phasors must rotate along with vector  $v$  for an equivalent space vector  $v$  in dq form. It can be seen that from Figure 2.7 that it is possible to convert the stationary  $\alpha\beta$  phasors into rotating dq phasors. The rotating frequency needs to be integrated within the transformation to ensure that it rotates along with the space vector  $v$ . It is achieved through the use of angle  $\theta$  which indicates the displacement of d-axis from

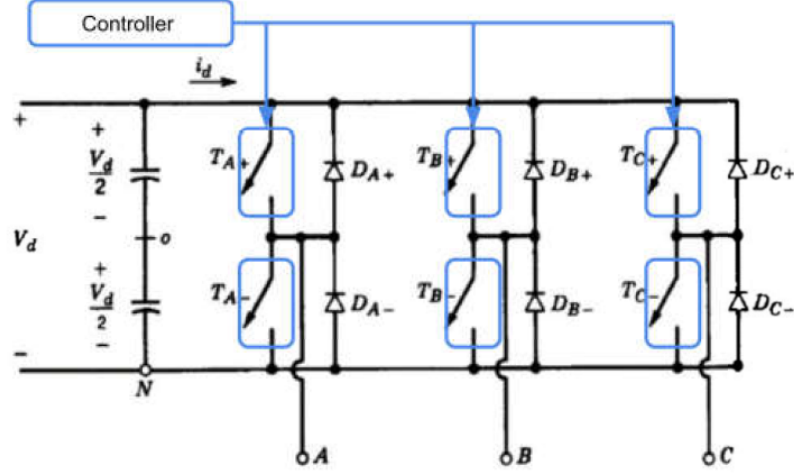


Figure 2.3: Single Line Diagram of VSC [48]

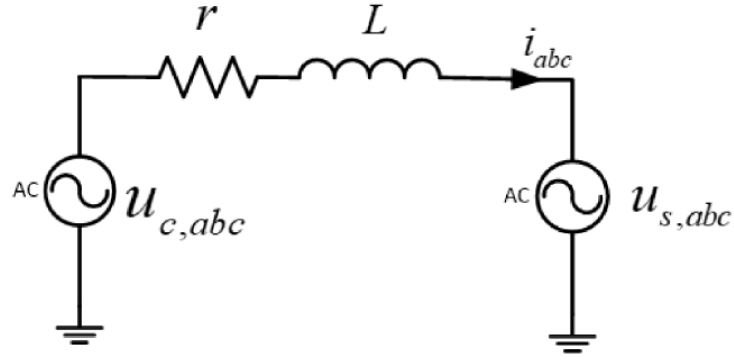


Figure 2.4: Simple circuit of a phase reactor [48]

the  $\alpha$ -axis at time  $t_i$ . The Park transformation is explained in detail through the following equations.

$$\theta = \omega_s t_s \quad (2.5)$$

$$\begin{bmatrix} u_s^d \\ u_s^q \end{bmatrix} = [T_{dq}] \begin{bmatrix} u_\alpha \\ u_\beta \end{bmatrix} = [T_\theta] \begin{bmatrix} u_a \\ u_b \\ u_c \end{bmatrix} \quad (2.6)$$

$$[T_{dq}] = \begin{bmatrix} \cos(\theta) & \sin(\theta) \\ -\sin(\theta) & \cos(\theta) \end{bmatrix} \quad (2.7)$$

$$[T_\theta] = \frac{2}{3} \begin{bmatrix} \cos(\theta) & \cos(\theta - \frac{2\pi}{3}) & \cos(\theta + \frac{2\pi}{3}) \\ -\sin(\theta) & -\sin(\theta - \frac{2\pi}{3}) & -\sin(\theta + \frac{2\pi}{3}) \end{bmatrix} \quad (2.8)$$

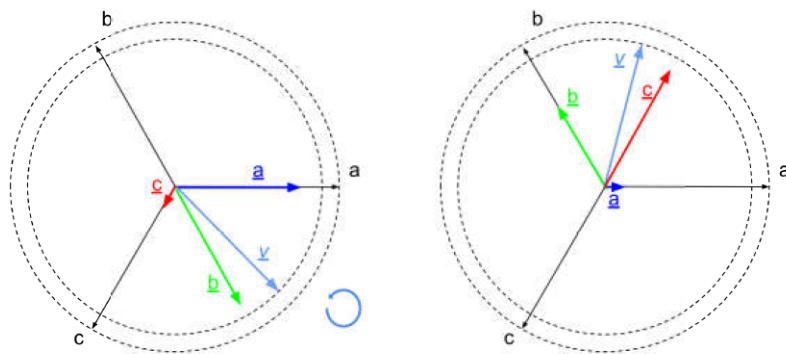


Figure 2.5: Phasors in the abc frame for  $t=t_1$  and  $t=t_2$  [48]

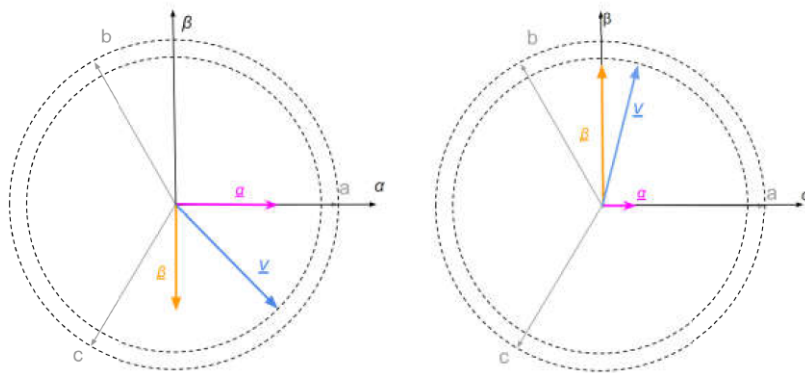


Figure 2.6: Phasors in the  $\alpha\beta$  frame for  $t=t_1$  and  $t=t_2$  [48]

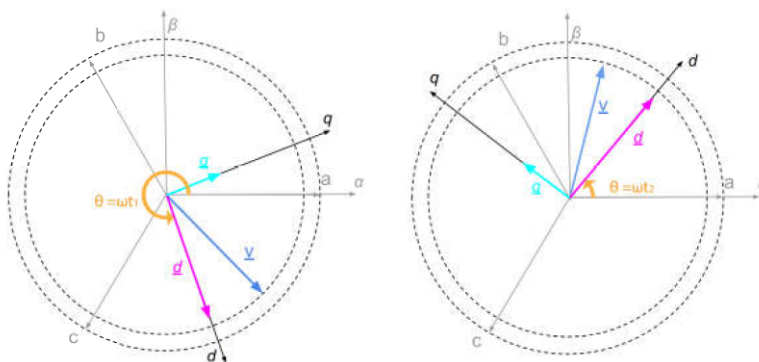


Figure 2.7: Phasors in the dq frame for  $t=t_1$  and  $t=t_2$  [48]

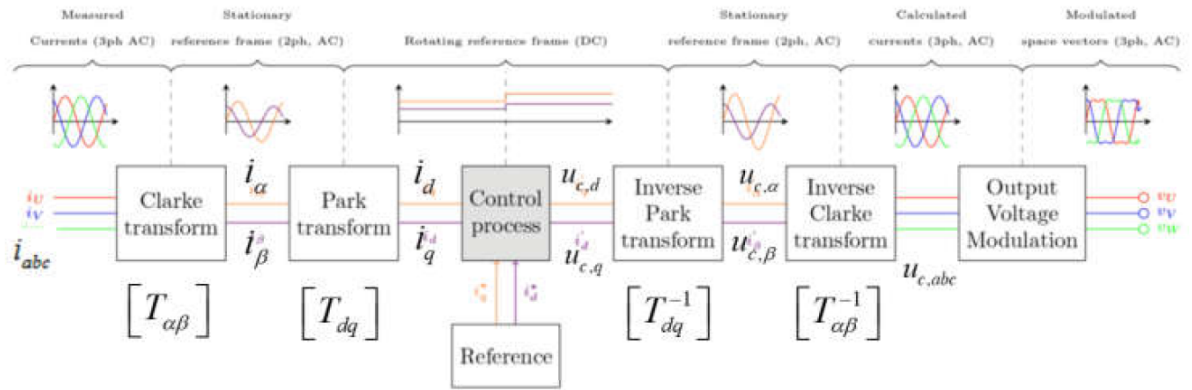


Figure 2.8: The steps of the transformation [48]

### Application

The control for the VSC is developed in the dq frame. As a result, the grid's measurements need to be transformed from abc to dq. Similarly, the output values from the controller are transformed back into abc from dq frame. The sequence is explained in Figure 2.8.

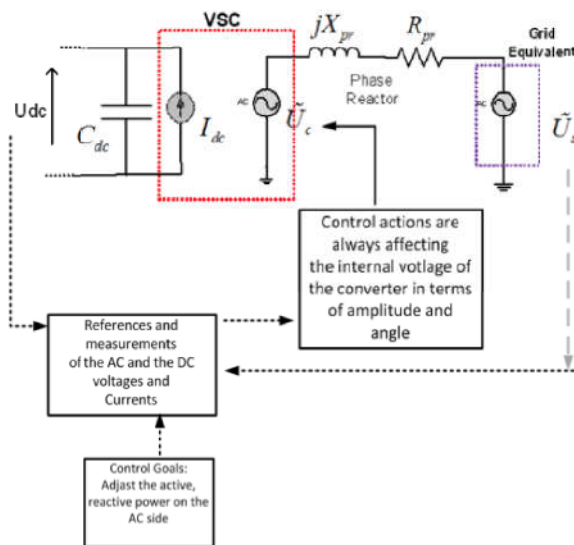


Figure 2.9: Diagram of the control architecture [48]

### 2.6.3. Control Loops

The control loops that process the signals are explained in this section. The main architecture of the controller can be seen in Figure 2.9. It can be seen that the grid's measurements along with goals of the converter provide the necessary information for the operation of the controller. The operation of the Phase Lock Loop (PLL) and current controller loops is vital for the overall operation.

#### Phase Lock Loop Controller

The equations below show that it is beneficial to align the d-axis to the space vector as it allows the decoupling of active and reactive power. This allows the active and reactive power of the

inverter to be controlled separately using the d and q component of the current respectively. The PLL is essentially a control module that uses a PI controller. The module locks the angle delta of the grid voltage such that the q-axis component of the grid voltage is zero in the rotating dq reference frame. In such a case, the magnitude of the grid voltage vector is equal to the d-axis voltage. The control block of the PLL is shown in Figure 2.10[51] and it can be seen that the angle delta is necessary for the transformation and inverse transformation of current and voltage.

$$P = u_s^q i_{pr}^q + u_s^d i_{pr}^d = u_s^d i_{pr}^d \tag{2.9}$$

$$Q = u_s^q i_{pr}^d + u_s^d i_{pr}^q = -u_s^d i_{pr}^q \tag{2.10}$$

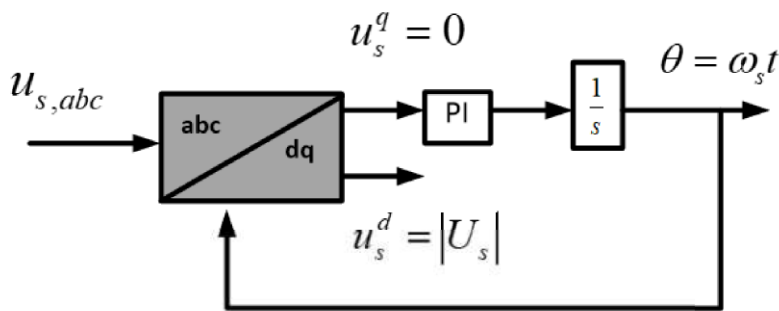


Figure 2.10: Control Block of the PLL [48]

For the accurate operation of the controller, it is vital that the PLL operation is stable and robust. If the PLL becomes unstable, the transformations are no longer accurate leading to the controller being subsequently unstable leading to a tripping of the VSC as it cannot follow the angle of the grid voltage anymore. The presence of grid harmonics is a common cause of PLL instability.

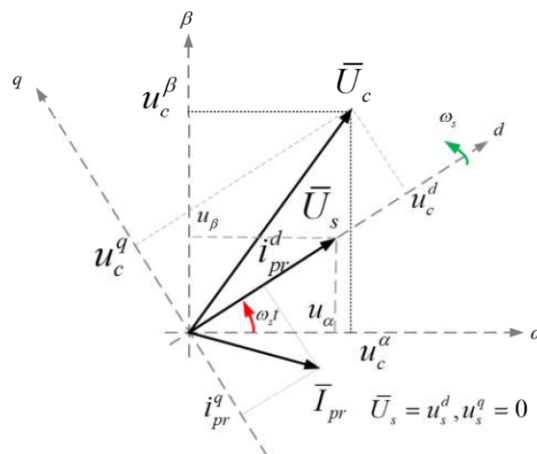


Figure 2.11: Operation of PLL[48]

**Inner controller**

The inner controller in the VSC controller is a current based controller. The output current of the VSC is controlled through the control of internal voltage as shown in Figure 2.12. A more

stable way of applying the controller is through looping the output current  $i_{dq}$ . This can be done by regulating the internal voltage of the converter  $U_{c-dq}$  through an inner controller to achieve the set point current  $i_{dq}$  as shown in Figure 2.13.

$$u_{c,d} - u_{s,d} = ri_d - \omega Li_q + L \frac{d(i_d)}{dt} = ri_d - \omega Li_q + sLi_d \quad (2.11)$$

$$u_{c,q} - u_{s,q} = ri_q - \omega Li_d + L \frac{d(i_q)}{dt} = ri_q + \omega Li_d + sLi_q \quad (2.12)$$

$$i_d = \frac{u_{c,d} - u_{s-d} + \omega Li_q}{r + sL} \quad (2.13)$$

$$i_q = \frac{u_{c,q} - u_{s-q} - \omega Li_d}{r + sL} \quad (2.14)$$

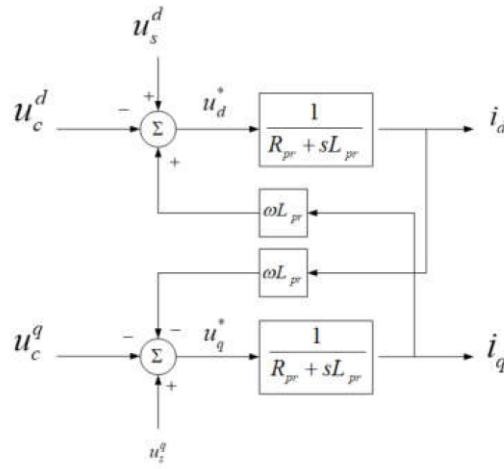


Figure 2.12: The open Loop VSC [48]

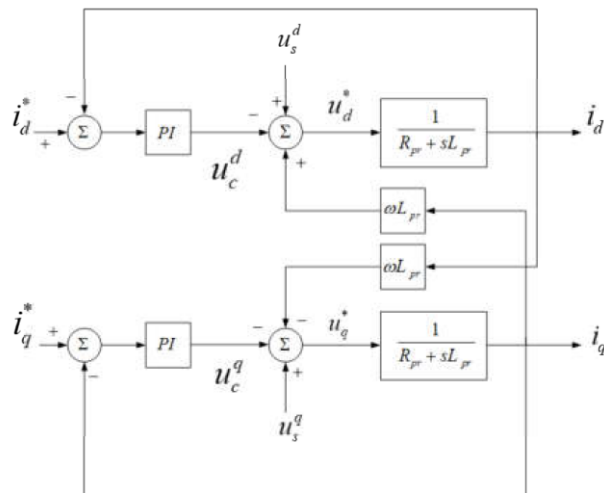


Figure 2.13: The closed loop VSC [48]

Outer Controller

The active and reactive power references define the reference values for the dq currents  $i_d$  and  $i_q$ . The active and reactive power references are in turn obtained from the grid requirements as explained below in the equations. The combined control loops is as shown in Figure 2.14

$$i_d^{ref} = (k_p + \frac{k_i}{s})(P_{ref} - P) \tag{2.15}$$

$$i_q^{ref} = (k_p + \frac{k_i}{s})(Q_{ref} - Q) \tag{2.16}$$

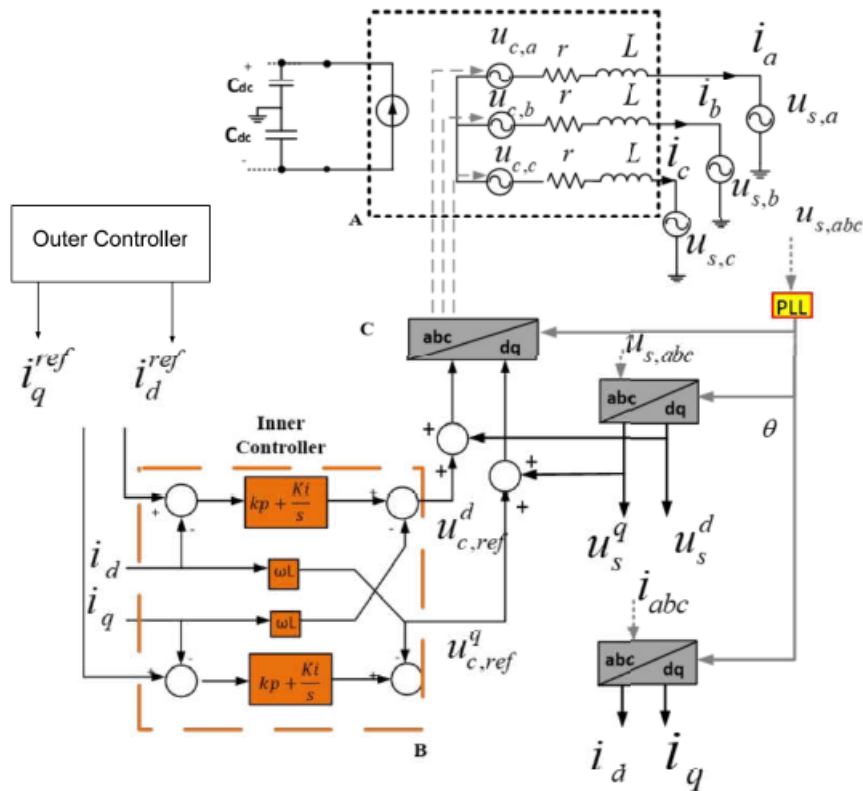


Figure 2.14: Overview of the control loops of the VSC [48]



# Methodology and Implementation in RTDS

## 3.1. CIGRE Model

### 3.1.1. Background

The CIGRE model used in the thesis is a benchmark model developed by CIGRE Task Force C6.04.02 [52]. The diverse nature of the distributed energy systems is a significant challenge for the testing and integration of DER and Smart Grid technology. The intention of the benchmark model is to provide a framework for analysis and validation of the developed methods and techniques for Network Integration of Renewable and Distributed Energy Resources.

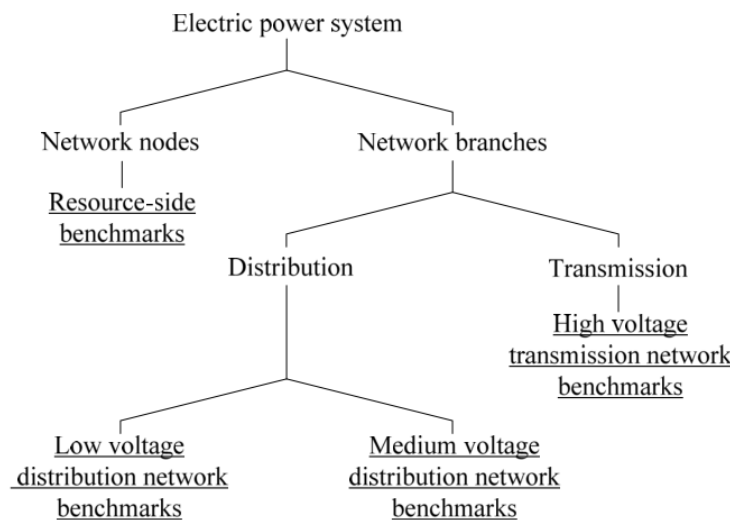


Figure 3.1: Hierarchy for identifying benchmarks [52]

The framework was developed by defining a hierarchical structure of four levels as depicted in Figure 3.1. This framework helps to distinguish transmission networks and distribution networks. However, the nature of the distribution networks can vary based on the voltage levels and local preferences. The model developed helps the researcher analyze the operation and control of distributed energy resources with increasing integration at lower voltage levels. With more intermittent renewable energy, it becomes more important to develop new methods and techniques to configure things like optimal power flow, unit commitment, energy management, security, frequency control, and voltage control. This benchmark was developed

in order to study the effects of interconnecting renewable and distributed energy resources with electric power systems and for detailed analysis of specific resource-side topologies and control strategies. For this purpose, a single benchmark configuration is desirable. This configuration can be adjusted using the recommended data to study resources with power ratings ranging from a few kW on low voltage distribution systems to hundreds of MW on high voltage transmission systems.

### 3.1.2. Medium Voltage Network Benchmark

The real life network used to develop the medium voltage (MV) network benchmark is a physical MV network in southern Germany which powers a small town and its surrounding rural area. The model was tweaked by reducing the number of nodes for the benchmark network to enhance user friendliness and flexibility while fully maintaining the characteristics of the network. The resulting benchmark model can be taken as a representative of a typical physical network in Europe. Some of the characteristics of the European MV Network Benchmark is as follows:

- **Structure:** The distribution feeders in the MV network is usually three phase with a nominal voltage of 20 kV and a system frequency of 50 Hz. The benchmark enables the configuration to either be a meshed or radial structure which is a feature of distribution networks.
- **Symmetry:** The physical network is usually built to be symmetrical by balancing the low voltage inputs along the MV lines. However, unbalances exist in reality and the benchmark enables the user to test that resilience of the network by introducing sources to create unbalance if necessary.
- **Line types:** The line types in the distribution network are modelled as underground cables. They are XLPE with round, stranded aluminum conductors and copper tape shields.
- **Grounding:** The nature of grounding depends on local preference and varies from country to country. It is generally modelled as ungrounded or impedance grounded.

### 3.1.3. Topology of MV benchmark network

The topology of the network used in the thesis is as shown in the Figure 3.2. The default CIGRE network has been tweaked a little to suit the needs of the project. It contains only one feeder operating at 20 kV with the switch S1 open. The details regarding the distribution network is provided in Table 3.1[52].

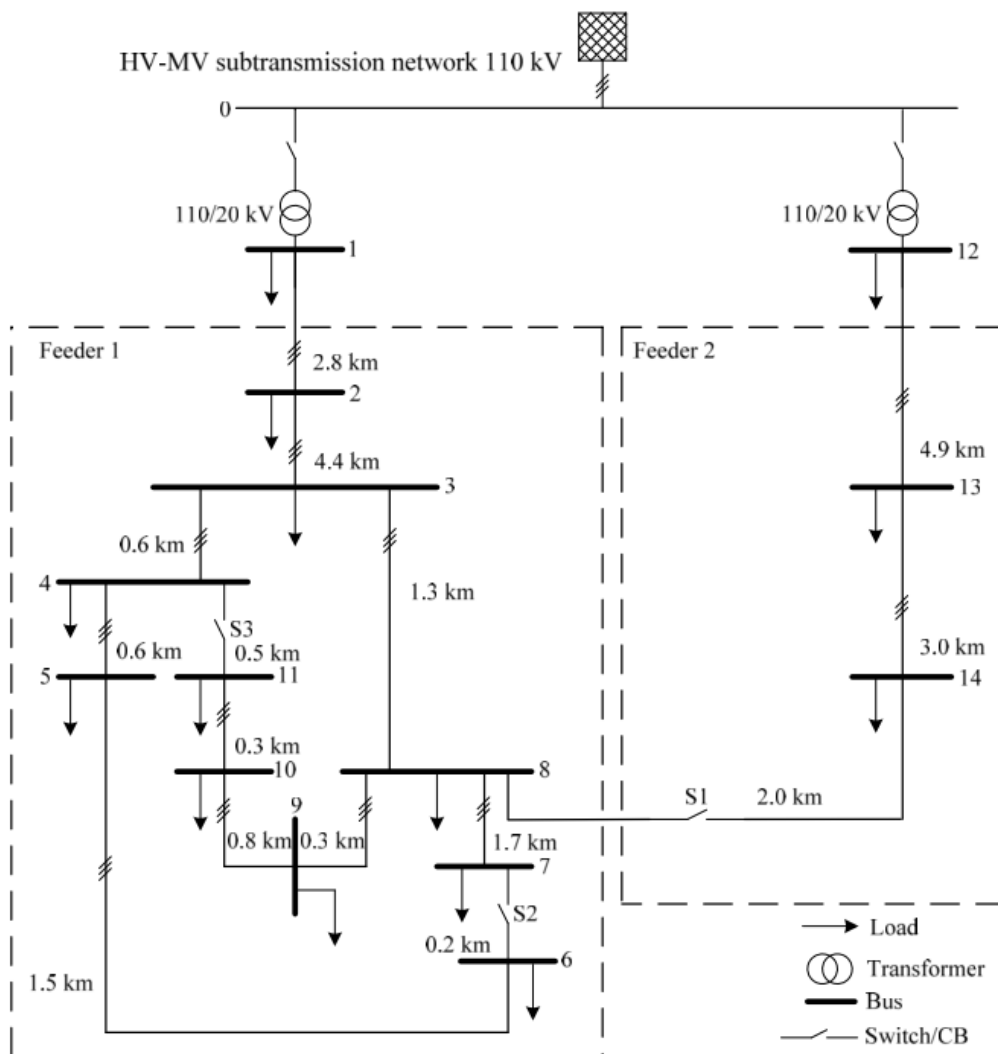


Figure 3.2: Topology of European MV distribution network benchmark 6.2.2 [52]

Line Segment	Node From	Node To	$R'_{ph}$ ( $\Omega/\text{km}$ )	$X'_{ph}$ ( $\Omega/\text{km}$ )	$B'_{ph}$ ( $\mu \text{ S}/\text{km}$ )	$R'_0$ ( $\Omega/\text{km}$ )	$X'_0$ ( $\Omega/\text{km}$ )	$B'_0$ ( $\mu \text{ S}/\text{km}$ )	$l$ (km)
1	1	2	0.501	0.716	47.493	0.817	1.598	47.493	2.82
2	2	3	0.501	0.716	47.493	0.817	1.598	47.493	4.42
3	3	4	0.501	0.716	47.493	0.817	1.598	47.493	0.61
4	4	5	0.501	0.716	47.493	0.817	1.598	47.493	0.56
5	5	6	0.501	0.716	47.493	0.817	1.598	47.493	1.54
6	6	7	0.501	0.716	47.493	0.817	1.598	47.493	0.24
7	7	8	0.501	0.716	47.493	0.817	1.598	47.493	1.67
8	8	9	0.501	0.716	47.493	0.817	1.598	47.493	0.32
9	9	10	0.501	0.716	47.493	0.817	1.598	47.493	0.77
10	10	11	0.501	0.716	47.493	0.817	1.598	47.493	0.33
11	11	4	0.501	0.716	47.493	0.817	1.598	47.493	0.49
12	3	8	0.501	0.716	47.493	0.817	1.598	47.493	1.30

Table 3.1: Connections and line parameters of European MV distribution network benchmark Line [52]

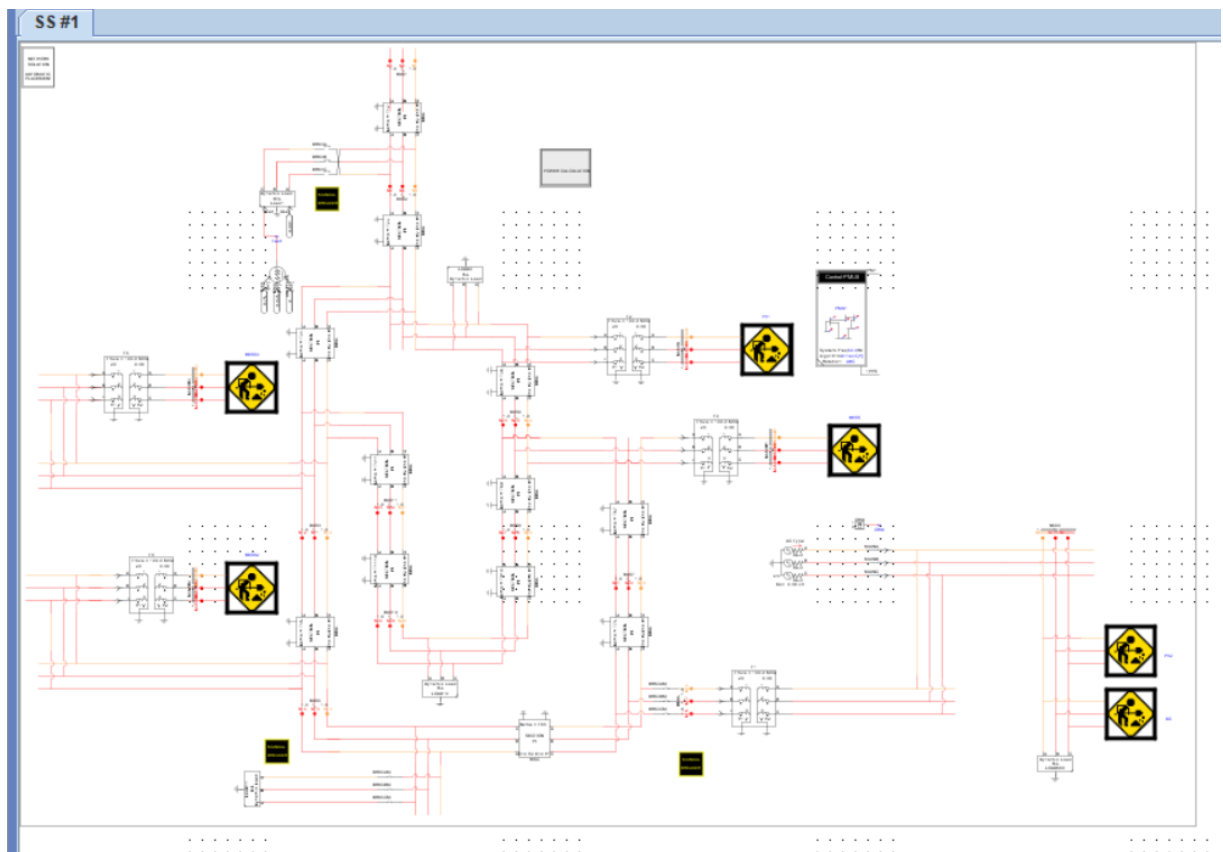


Figure 3.3: Benchmark network on RSCAD

The topology of the network described in Figure 3.2 was modelled on RSCAD and is as shown in Figure 3.3. This model includes the following:

1. A Diesel generator explained in detail in Generator model section
2. Two PV sources explained in detail in PV model section
3. Three battery sources explained in detail in the Battery model section

The sources mentioned above (PV/DG/Battery) are modelled as average models instead of the small time step models usually associated for power electronic interfaces at the grid level. Small simulation time steps (less than 4 micro secs) are normally used to accurately model the high switching frequency transients in modern power electronic interfaces. In a distribution network with many distributed energy resources (DERs), the computational burden of such a detailed small time step model places a limitation on the size of the distribution network that can be simulated. To overcome this problem, DERs were modelled as DC/AC average models as shown in Figure 3.4. The DC/AC average model enables the user to integrate a DC source like PV or BESS to the AC grid. It sufficiently depicts the real and reactive power profile of the converter even if it neglects the effect of the switching devices. As a result, the average model requires much less computational resources than the fully switched small time step models and enables the user to build large scale distribution networks without much limitation.

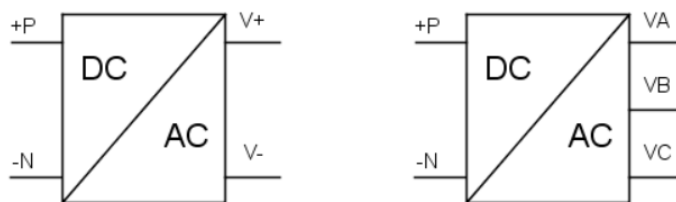


Figure 3.4: Single and Three Phase Average Models for DC sources

### 3.2. Underground cables

The underground cables in the distribution network were modelled as PI sections as shown in Figure 3.5. PI section model is not the default method to represent underground cables in the RTDS system but it is a useful tool to accurately represent a line based on the length of the line. According to the RTDS website, if the length of the line is less than 15 km, the line can be represented using a PI section. This is based on the distance travelled by light during a 50 usec time step which is approximately found to be 15 km.

#### PI-SECTION MODEL

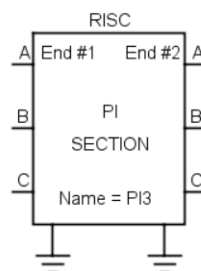


Figure 3.5: PI section model in RSCAD

### 3.3. Generator model

The generator model used in the distribution network is a simple model which contains a rotating machine along with a exciter (library model) and a governor which is user defined. The user defined governor model enables the user to change the droop of the generator which is a useful feature to have in comparison studies. The generator is then connected to the distribution network through a breaker as shown in Figure 3.6.

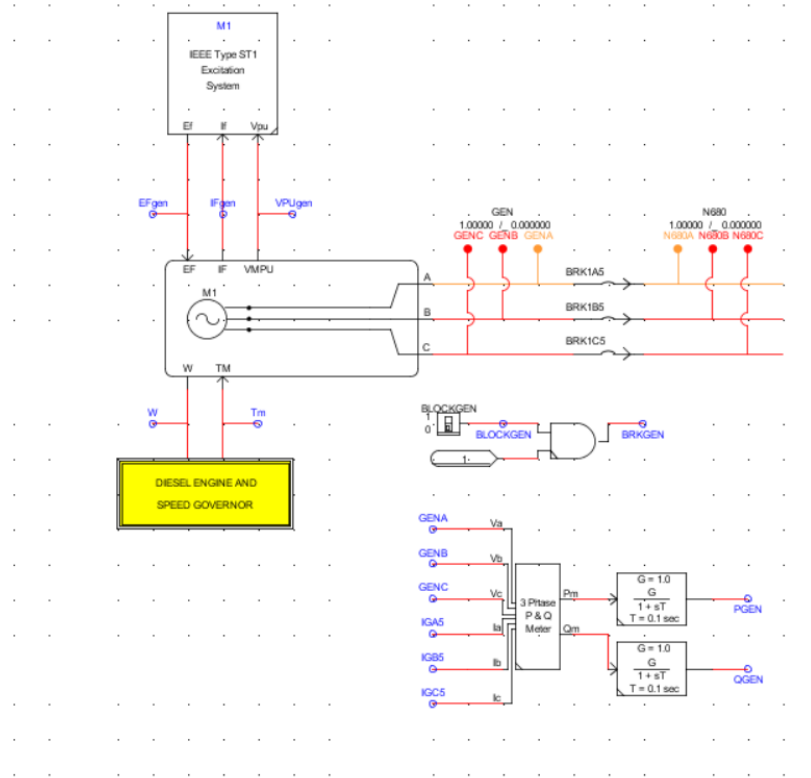


Figure 3.6: Generator model in RSCAD

### 3.4. Battery model

The battery model in the distribution network consists of a battery source modelled according to [53] which is connected to a DC/AC converter average model and integrated with the AC grid network with a breaker and transformer as shown in Figure 3.7 and Figure 3.3.

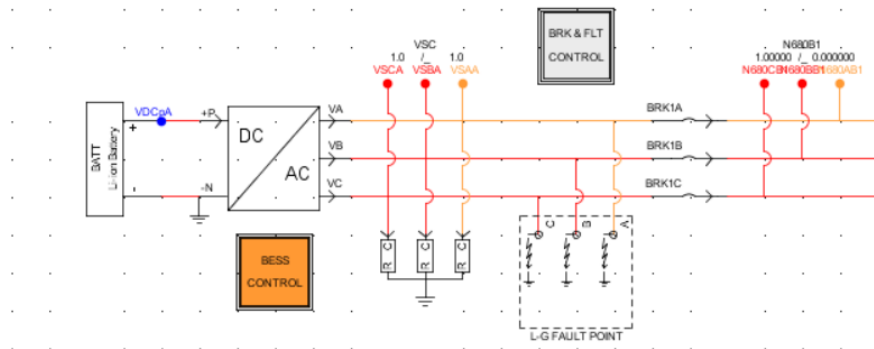


Figure 3.7: Battery model in RSCAD

The set points for the DC/AC battery converter is taken care by the BESS control block as shown in Figure 3.7. The inner workings of the BESS control block is shown in Figure C.1. A representation of the control model is shown below in 3.8

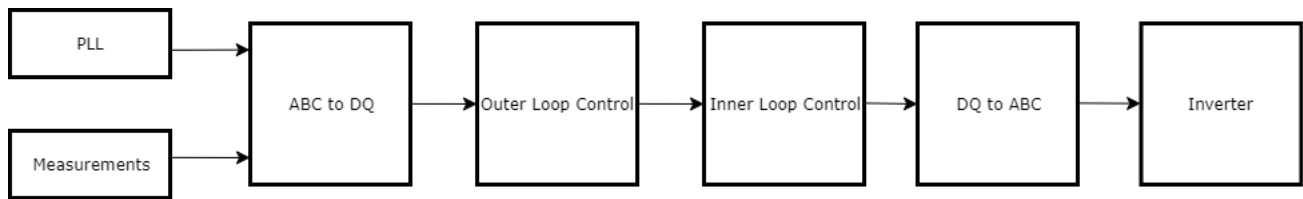


Figure 3.8: Battery control representation

The BESS control block has different sub blocks in it which take care of different functions. They are as follows:

1. PLL block: This block is important to ensure that the voltage is always aligned with the d axis of the converter as explained in Chapter 2.
2. abc to dq block: These blocks are used to convert the measured abc values in the network to dq frame for use in the control schemes.
3. Measurement & Start up block: These blocks are used to measure current and voltage values from the network and provide reference points for the control logic blocks
4. Outer Loop control block: This block is used to provide current reference points based on the real and reactive power requirements from the distribution grid
5. Inner Loop dq control block: This block converts the current based reference value into dq voltage values
6. Average Control Voltage and Current block: The dq voltages values are converter into abc domain in this block and used as set points for the DC/AC converter.



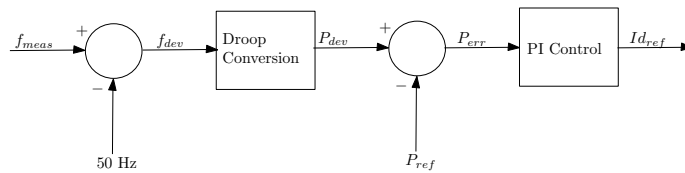


Figure 3.11: Primary Frequency control

### 3.6.2. Peak Shaving

Figure 3.12 describes the Frequency & Peak-shaving integrated control algorithm used in the model. It is an upgrade on the primary frequency control model. In this model, the peak shaving component is integrated through a factor which is controlled by PS block. The additional component is calculated by deriving the instantaneous difference between power generated and consumed which can be interpreted as a signal from a DSO in real life. The peak shaving component and the primary frequency component are calculated in parallel and taken into consideration to derive the  $I_d$  component. As with the previous algorithm, the  $I_q$  component is assigned to be zero since it does not involve reactive power. The implementation in RSCAD is illustrated in C.4

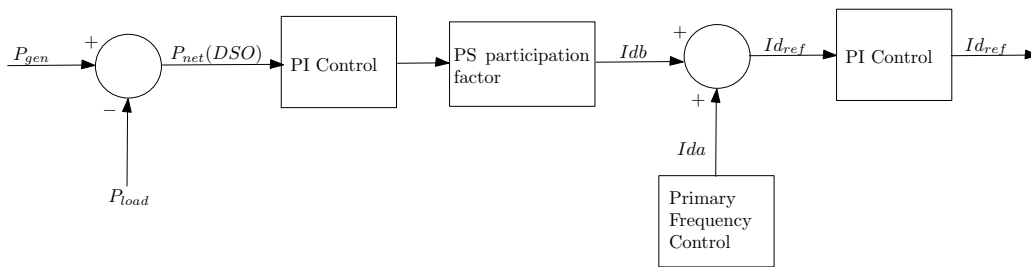


Figure 3.12: Primary Frequency control & Peak Shaving

### 3.6.3. Integrated control

The control scheme for integrated control is as shown in the Figure 3.13 with the RSCAD implementation shown in Figure C.5 . In this control scheme, both voltage and frequency are parameters to be controlled. The frequency and voltage control schemes is combined to provide an integrated control scheme. Frequency is controlled using the scheme earlier seen in the peak shaving algorithm. As for the voltage control, the voltage on the bus is measured and then compared with the nominal value to identify the deviation. This deviation is then used to derive the  $I_q$  component as shown in the Figure 3.13.

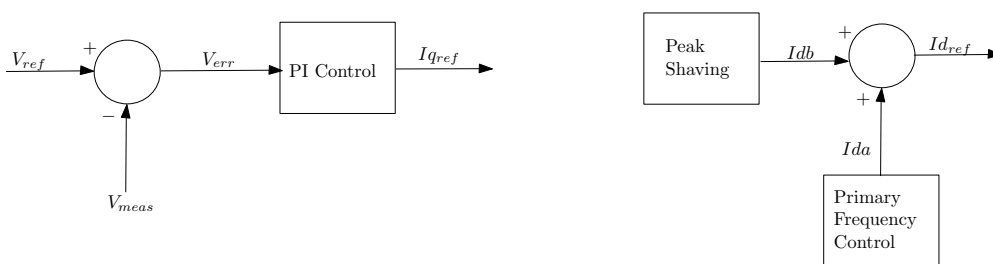


Figure 3.13: Integrated control

### 3.6.4. Integrated control with multiple BESS

The control scheme for integrated control with multiple BESS is as shown in the Figure 3.14 with the RSCAD implementation shown in Figure C.6 .The difference from the previous scheme comes from the SOC factor while calculating the droop for the battery systems involved. In this control scheme, the droop of each BESS is calculated based on the SOC of the

BESS involved. As a result, the contribution of a BESS towards integrated control will decrease when the SOC of a particular BESS is low. This is done to optimize the performance of a portfolio of a BESS by ensuring that as many BESS stay operationally as possible to maintain energy capacity of the portfolio.

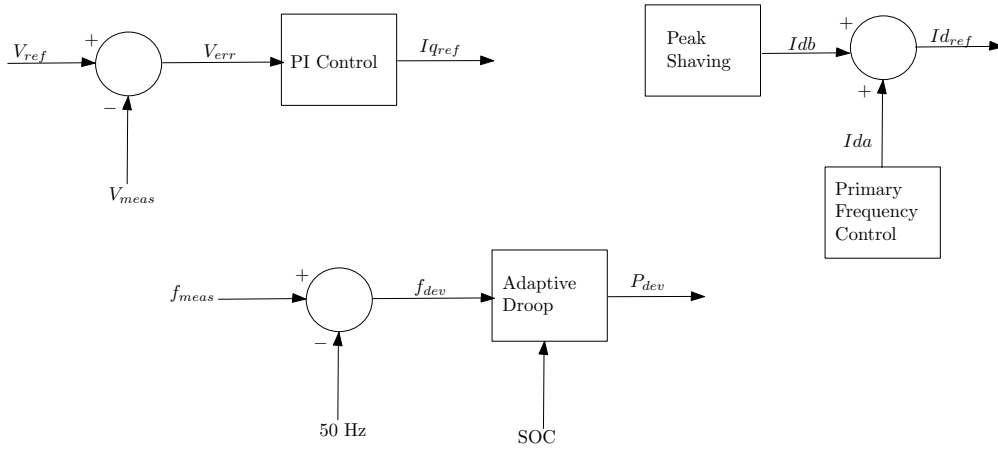


Figure 3.14: Integrated control with multiple BESS

### 3.6.5. Integrated control with time delay

This control algorithm is designed to test the influence of time delay with respect to the robustness of the system. The focus of the time delay in this case is at the sensor level. To introduce time delay in the control algorithm of the BESS, a variable user defined block has been introduced before measuring the frequency from the grid as shown in Figure 3.15 with the RSCAD implementation shown in Figure C.7. This will in turn lead to a delay in calculating the droop of the BESS

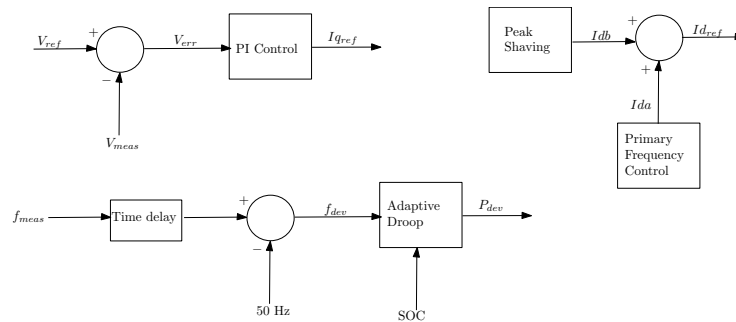
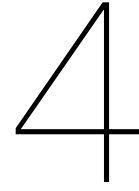


Figure 3.15: Integrated control with time delay

### 3.6.6. Micro-grid voltage control

The micro-grid voltage control scheme focuses more on the voltage of the system as opposed to the frequency parameter in the earlier cases. The purpose of this control algorithm is to demonstrate the usefulness of a BESS when it comes to black starts due to emergencies. The BESS forms the grid in micro grid mode and it measures the voltage of the network and compares it with the nominal value of 480 V to create the  $i_q$  reference point. This is similar to the voltage control scheme explained in Figure 3.13. The RSCAD implementation is as shown in Figure C.8. The control scheme shown in Figure C.9 describes the Voltage control algorithm used in grid connected conditions. The difference between the  $V_{ref}$  and the deviation in grid voltage is used to derive the  $I_q$  component. The  $I_d$  component is assigned to be zero to isolate it as voltage control.



# Results & Discussions

To achieve the goal of demonstrating integrated control in BESS, different control schemes were tested and compared in terms of performance with respect to frequency control. This section will focus on describing the performance of the different controllers and the subsequent results accompanied by a short analysis.

## 4.1. Network Scenarios

Three network scenarios will be tested in this thesis. Based on active power contribution, they are as follows:

1. **Low RES penetration:** 30 % PV & 70 % rest (DG + BESS)
2. **Medium RES penetration:** 50 % PV & 50 % rest (DG + BESS)
3. **High RES penetration:** 98 % PV & 2 % rest (DG + BESS)

The purpose of the network scenarios is to enable the user to observe and analyze the behaviour of the BESS in different levels of renewable penetration. The location of PV in the network is not the focus of this thesis.

## 4.2. Applications

The above-mentioned network scenarios will be tested through a controller with a step load of 30% (to simulate a loss of generation source or a sudden increase in demand) at 1.5 s for:

1. Primary Frequency control (Traditional Control Scheme)
2. Peak Shaving (PS) services & Primary frequency control
3. Integrated control for Primary frequency control
4. Primary Frequency Control with Time Delay
5. Primary Frequency Control with Two BESSs
6. Primary Frequency Control with Three BESSs
7. Voltage control (Micro-grid)

The Integrated control method is also tested for a step load disturbance of 0.2 MW and 0.2 MVAR at 1.5 s.

### 4.3. Primary Frequency control (Traditional Control Scheme)

The active power output of the generator for different scenarios when subjected to a step disturbance of 0.3 MW at 1.5 s is as shown in Figure 4.1 and it can be easily seen that the power output of the generator is higher without the BESS since the generator needs to contribute more active power for frequency stability when subjected to the same step disturbance of 0.3 MW. It can also be seen that this trend holds true for different levels of RES penetration.

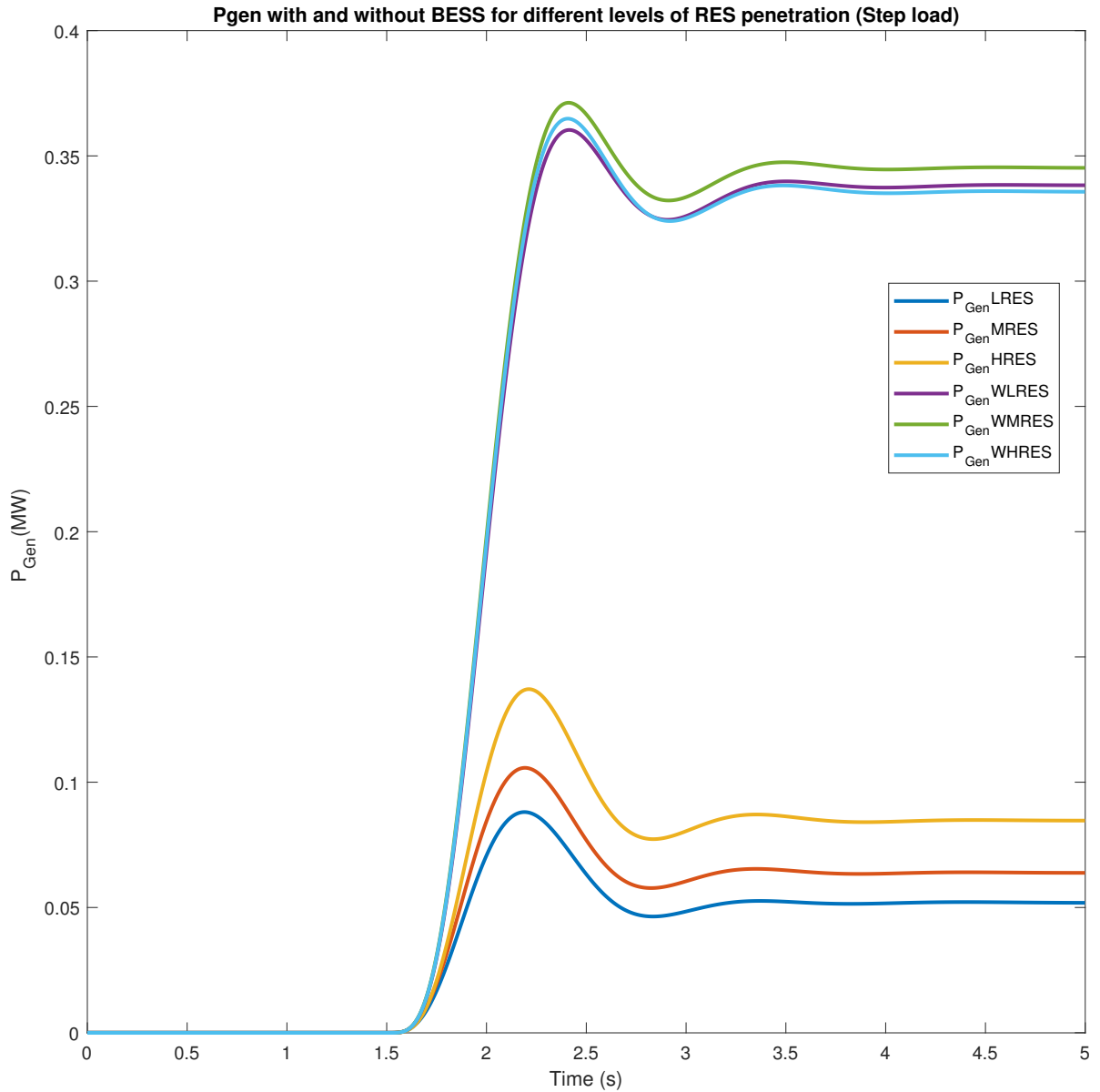


Figure 4.1: Primary Frequency Control with and without BESS - Step Load

#### 4.4. Peak Shaving (PS) services & Primary Frequency control

The figure shows the active power output of the BESS, Generator and the frequency of the system for different levels of peak shaving contribution when subjected to a step disturbance at 1.5 s. The peak shaving contribution refers to the contribution of power coming from the peak shaving +PFR algorithm for frequency control. It can be seen that the power contribution during primary frequency control is the highest when PS = 0. On the frequency front, it can be observed that the best transient response is for PS = 0.5 with the nadir being the lowest for PS = 0.1. As a result, it can be concluded that the best factor for PFR + PS contribution should be with PS = 0.5. The generator contribution is as expected as it offsets the different power output for BESS for different values of PS. The trend is observed to be the same for all levels of RES penetration.

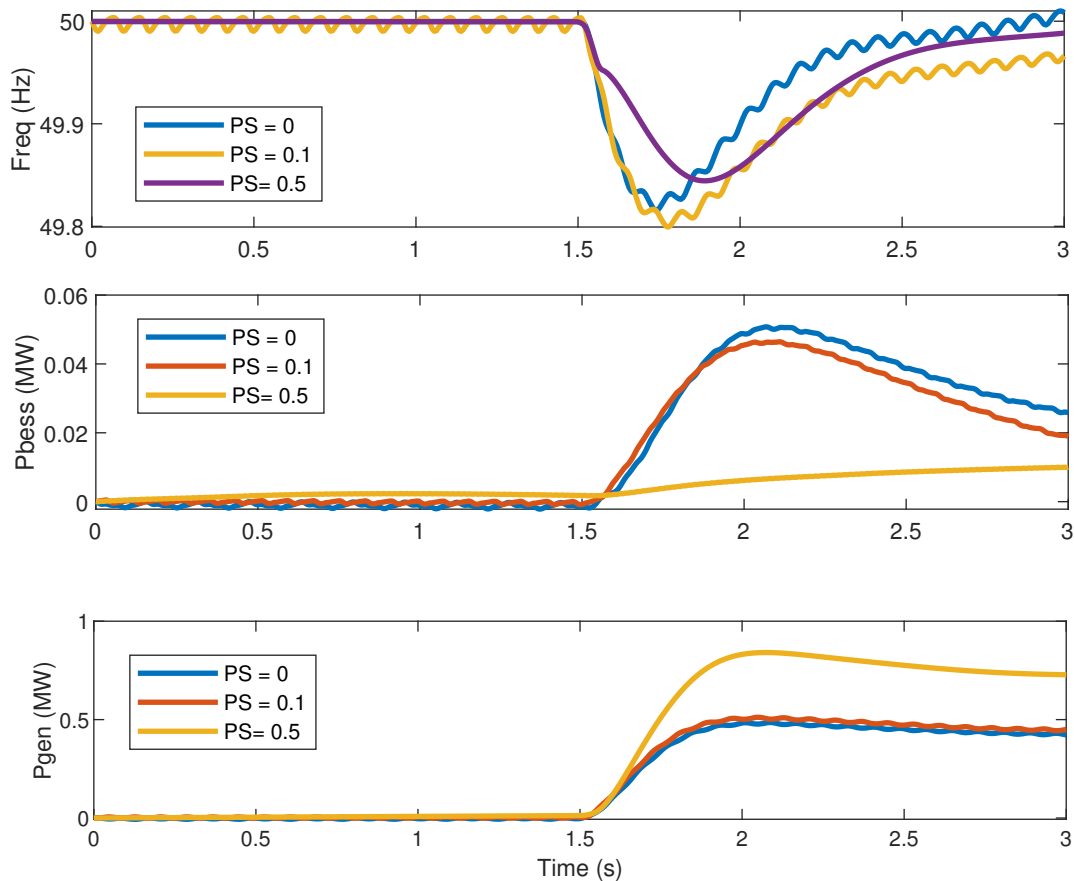


Figure 4.2: Peak shaving contribution

### 4.5. Integrated control for Primary Frequency control

Figure depicts the active power output of the BESS, Generator and the frequency of the system for different control schemes when subjected to a step disturbance at 1.5 s. The different control schemes are traditional PFR, Integrated and Peak shaving algorithms. On the frequency front, it can be seen that the integrated control algorithm is the best one in terms of robustness since it has the smallest settling time. The output of the generator is as expected as it offsets the BESS output. The trend is observed to be the same for all levels of RES penetration.

As seen from the above figures, a change in frequency measurement method was made. It was changed from a PMU block to a standard frequency meter (refer images below). This provides a better representation of the frequency response of the system as illustrated in the graphs above. Furthermore, the application of a low pass filter along with the frequency meter gives a smoother and better response in line with the power outputs. The power outputs of the BESS and generator complement each other.

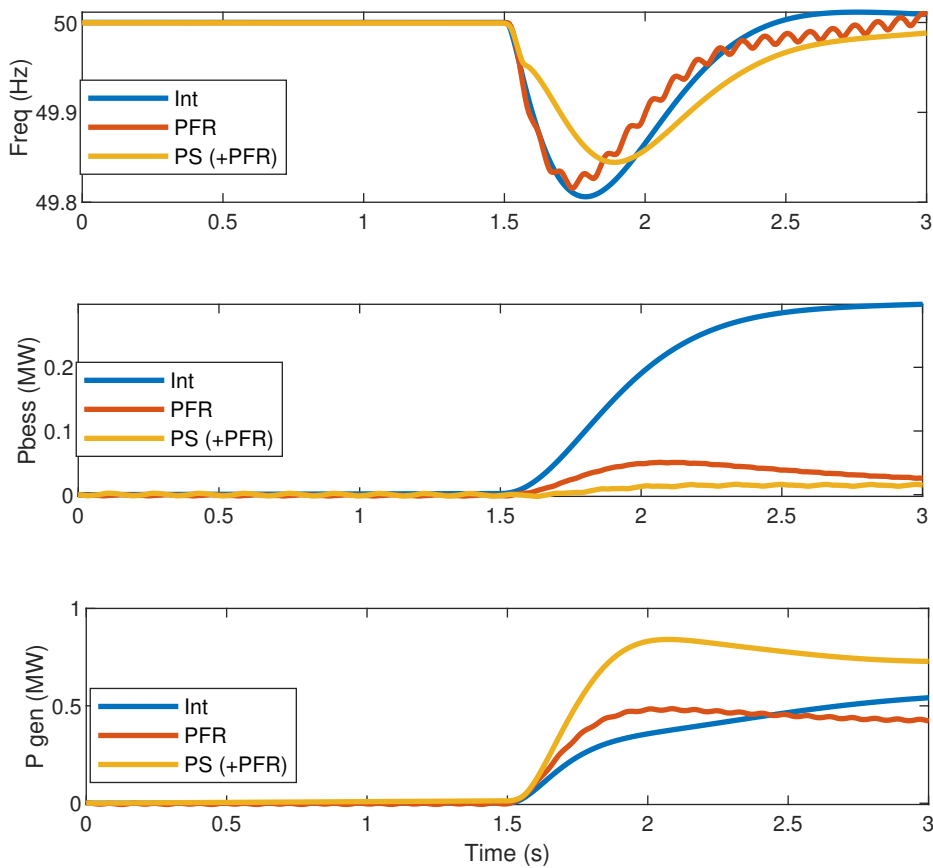


Figure 4.3: Different control schemes

## 4.6. Integrated control for Primary Frequency & Voltage Control

Figure 4.4 illustrates the response of the BESS in terms of active and reactive power output when subjected to a step load disturbance of 0.2 MW and 0.2 MVar at 1.5 s. It can be seen that both the frequency and voltage values are quickly stabilized after the disturbance at 1.5 s. The contribution of the BESS is split between the frequency and voltage control due to the inverter capacity limitation. As a result, there is a bigger contribution for frequency control as opposed to voltage control in this particular instance. The contribution can be improved by increasing the size of the inverter.

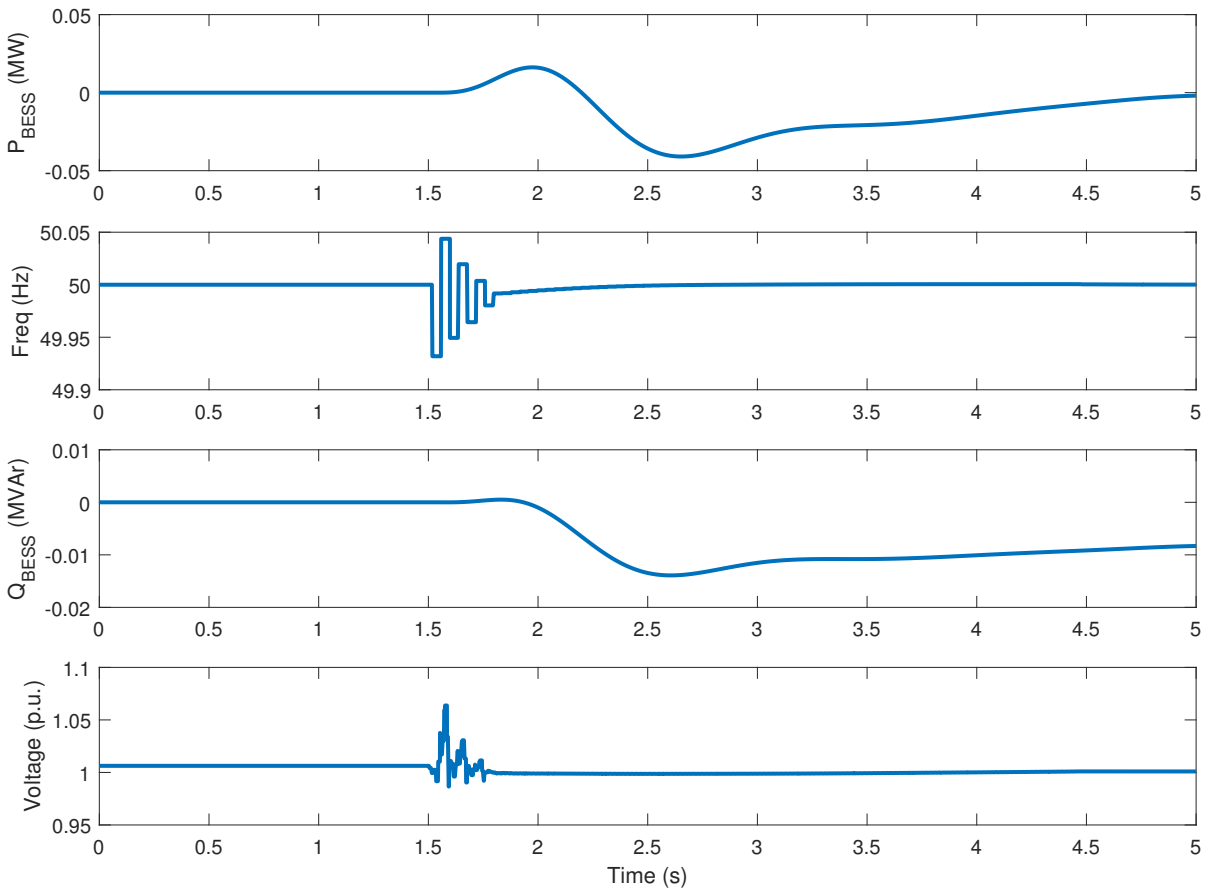


Figure 4.4: Integrated control for Primary frequency control & Voltage Control

## 4.7. Primary Frequency Control with Two BESSs

Figure 4.5 shows the performance of the two BESS systems BESS 1 and BESS 3 in tandem providing primary frequency control when subjected to a step disturbance of 0.3 MW at 1.5 s. Two test cases were tested in the study, the first case involved both the BESS systems starting with a SOC of 0.85 and the second case involved BESS 1 starting with SOC = 0.3 and BESS 2 starting with SOC = 0.85. It can clearly be seen that the power output of the BESS varies with starting SOC. This is because of the algorithm which has been defined to factor in SOC while calculating the droop value. The droop value is configured to be inversely proportional to the SOC value as explained in Chapter 3. As a result, a battery with a smaller SOC in this case BESS 1 will lead to a smaller contribution to the primary frequency control when the SOC of the battery is lower. This algorithm is very useful when an aggregator like a virtual power plant is managing a portfolio of batteries as it helps to deliver an optimal power output taking into consideration the state of charge of batteries thereby ensuring optimal power output and longer lifetime.

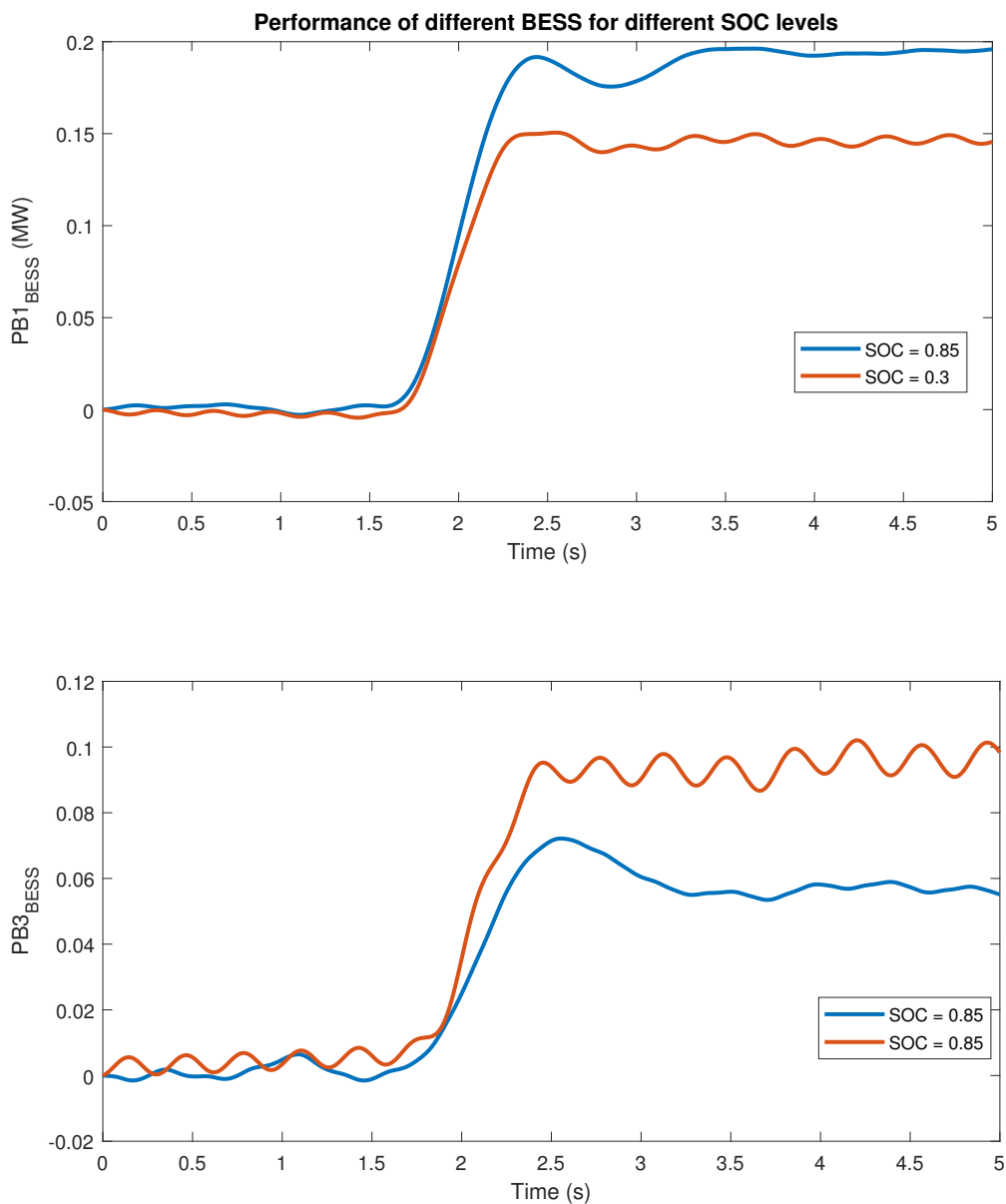


Figure 4.5: Integrated control with multiple BESS

## 4.8. Primary Frequency Control with Three BESSs

It was initially seen that the coordination of BESS becomes increasingly difficult as the number of batteries increase. This can be seen in Figure 4.6 with the frequency volatility suddenly increasing when the number of batteries change from two to three.

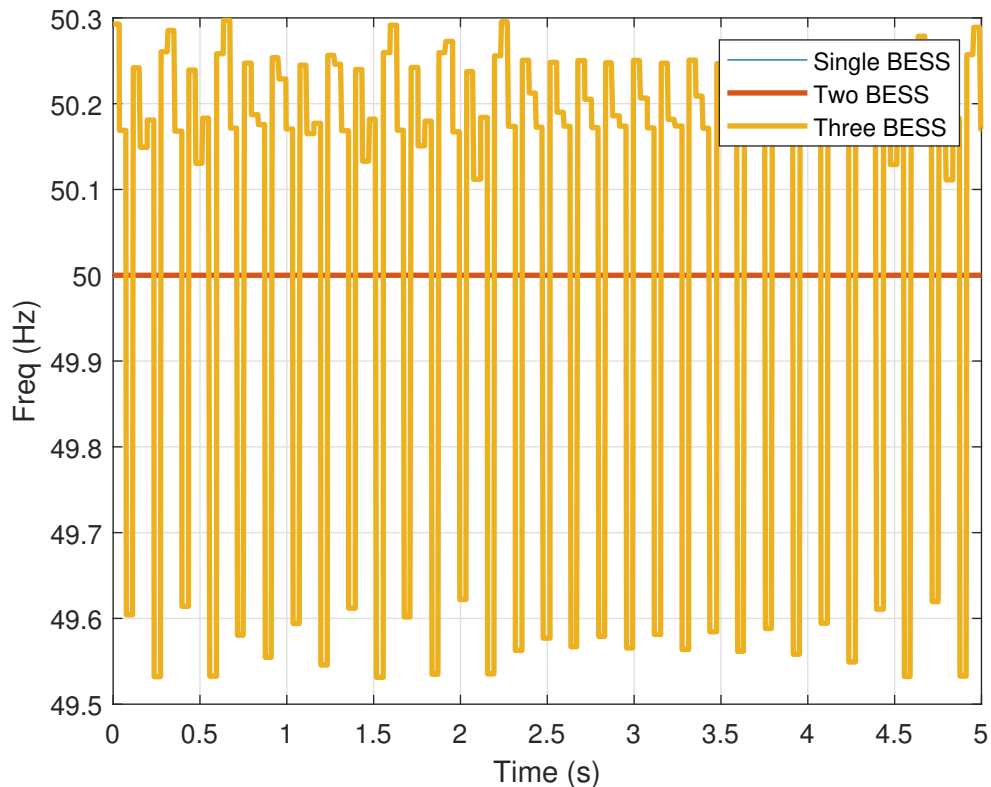


Figure 4.6: Frequency comparison for coordination of multiple BESS

The volatility of the frequency was solved in two parts. The sensors were upgraded to remove the noise in the measurements by passing it through a low pass butterworth filter. This significantly reduced the frequency volatility as observed in Figure 4.7. In addition to this, the power output of the BESS systems were limited to avoid causing volatility. A comparison study for different levels of limitation was done to test the optimal value and it was found that the power output of the BESS should be limited to be 1.5 pu as shown in Figure 4.8. This shows that the BESS systems need to be reconfigured in terms of the power output if they want to participate as a part of a VPP system.

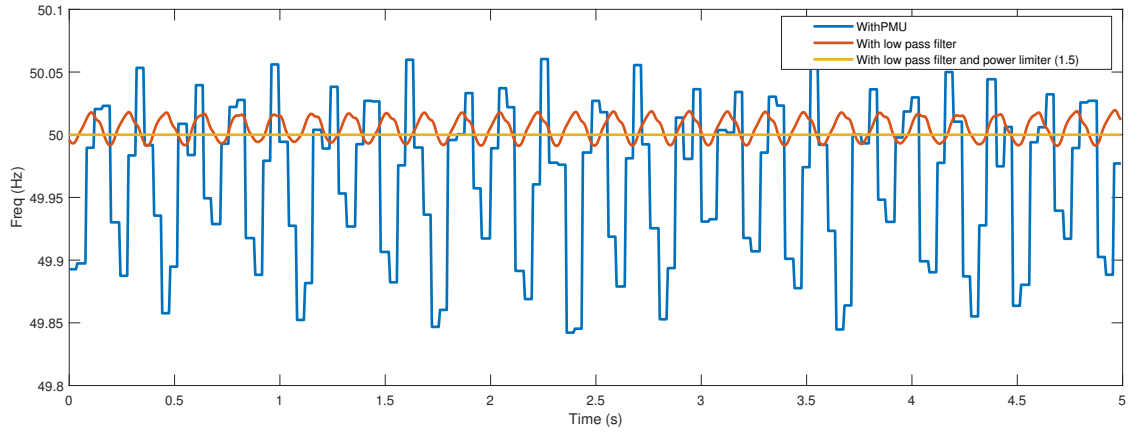


Figure 4.7: Comparison of frequency for different measurement techniques

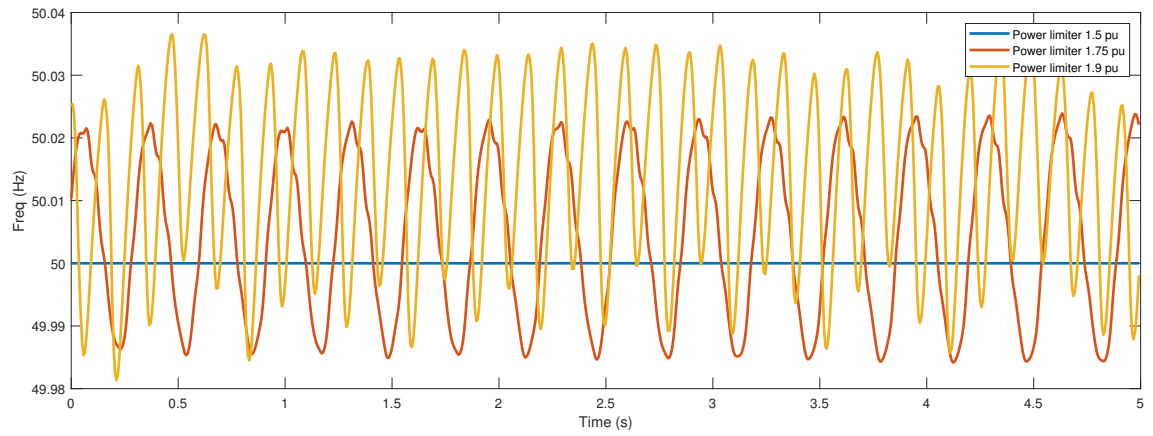


Figure 4.8: Comparison of frequency for different BESS power limits

## 4.9. Primary Frequency Control with Time Delay

The power output of the BESS system for different cases of sensor delay when subjected to a step disturbance of 0.3 MW at 1.5 s can be observed in Figure 4.9. It can be seen that the rise time and the steady state output is almost the same for different cases of sensor delay (0, 0.1, 0.3, 0.7 s). As a result, it can be concluded that a sensor or a communication delay of up to 0.7 s does not affect the robustness of the algorithm and BESS in terms of providing ancillary services to the distribution network.

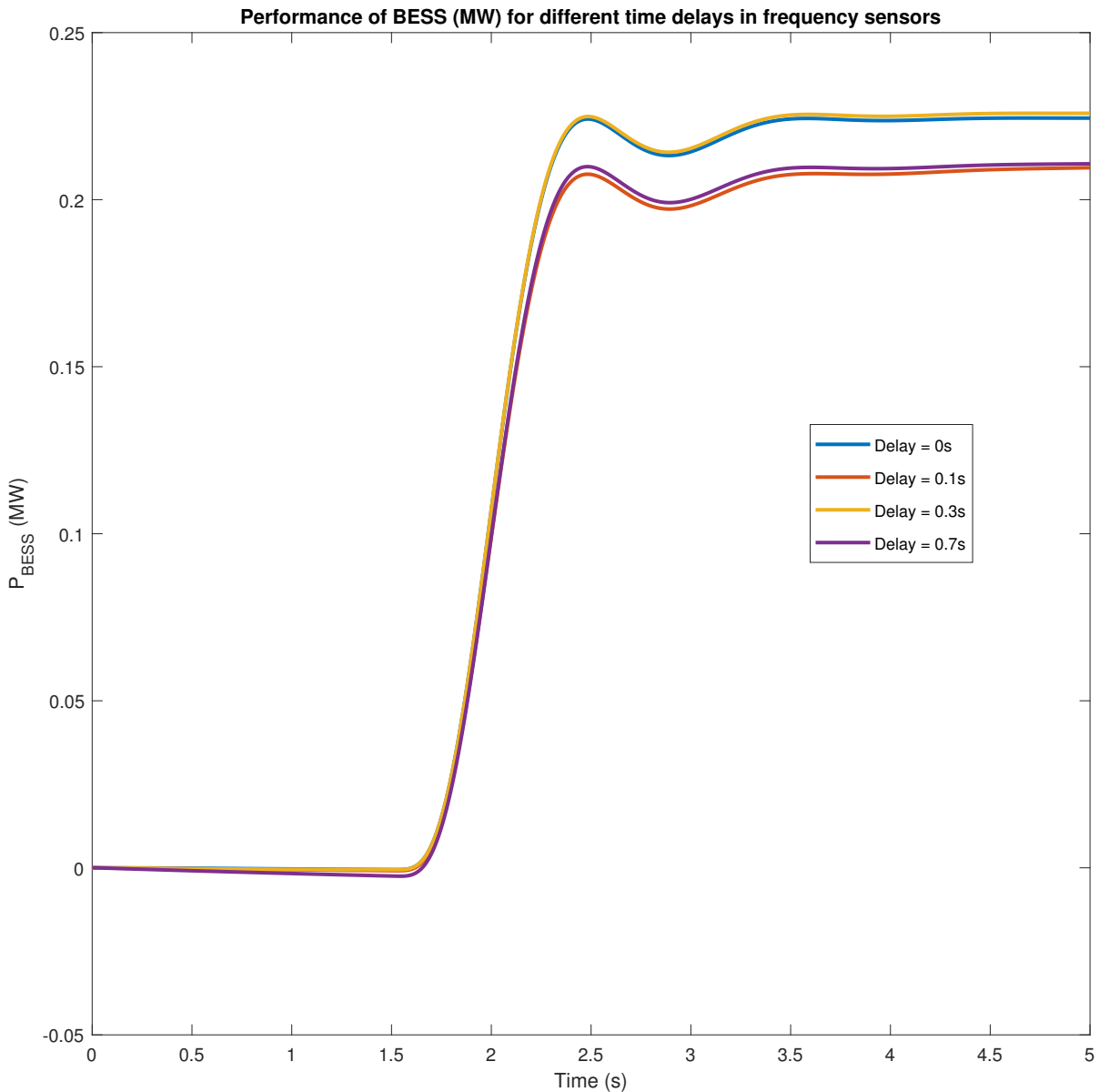


Figure 4.9: Integrated control with time delay

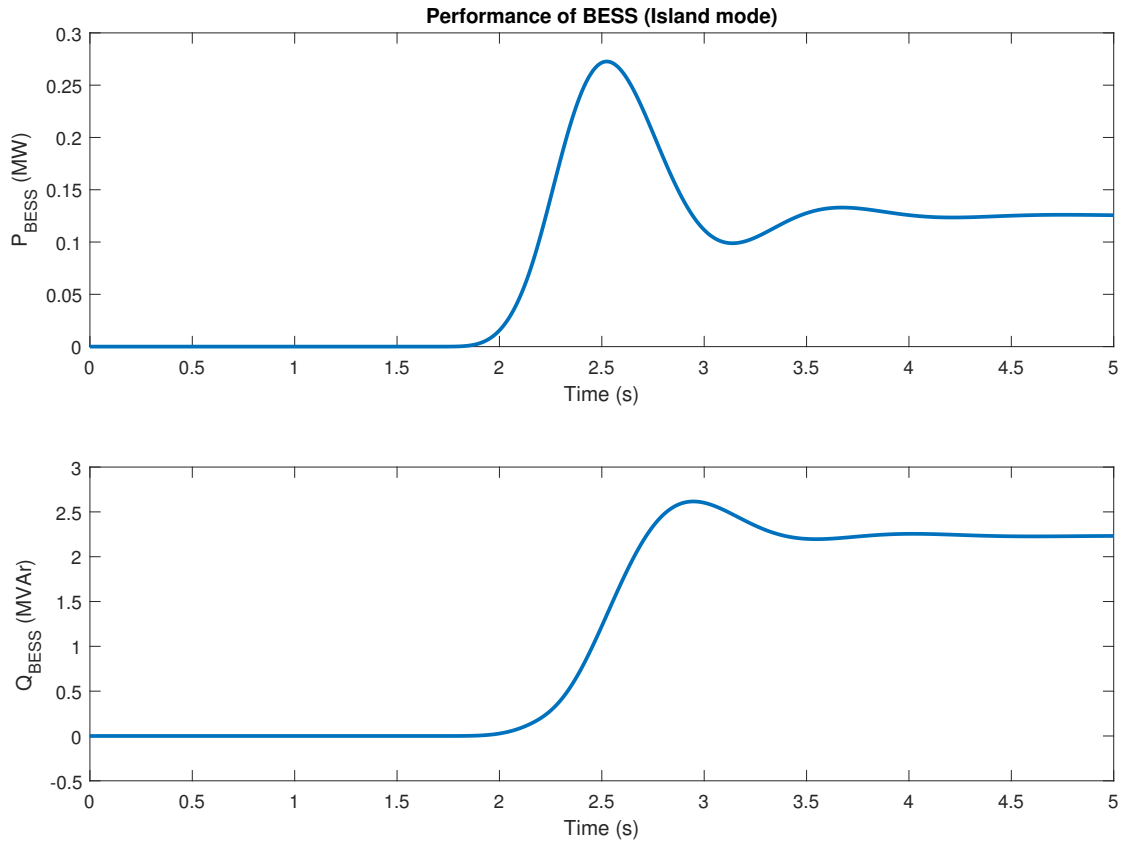


Figure 4.10: Micro-grid - Island mode

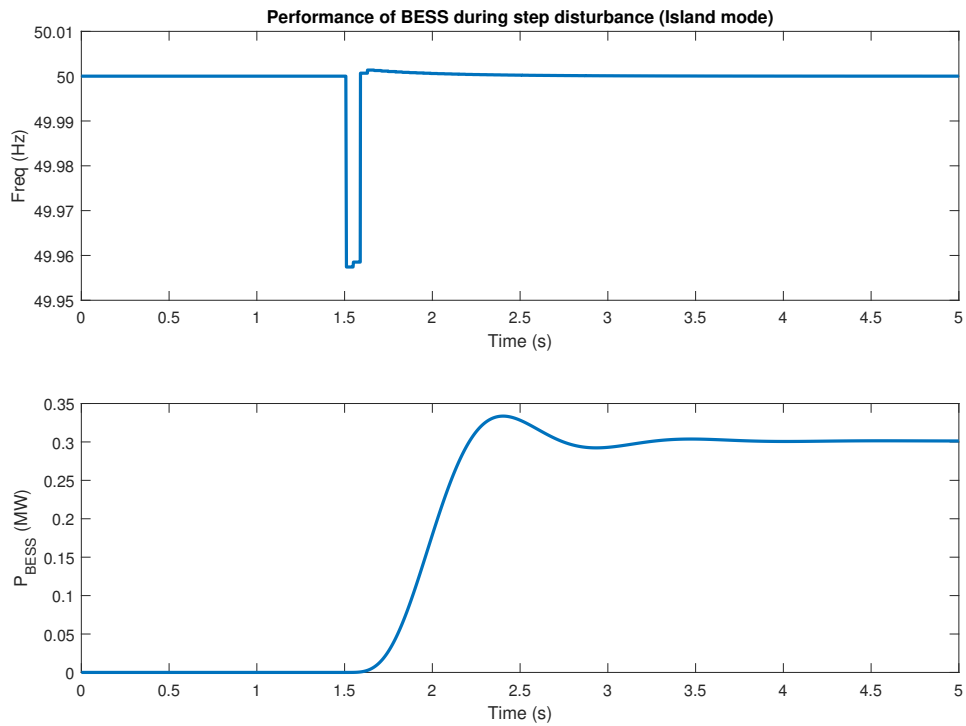


Figure 4.11: Micro-grid - Island mode (Step disturbance)

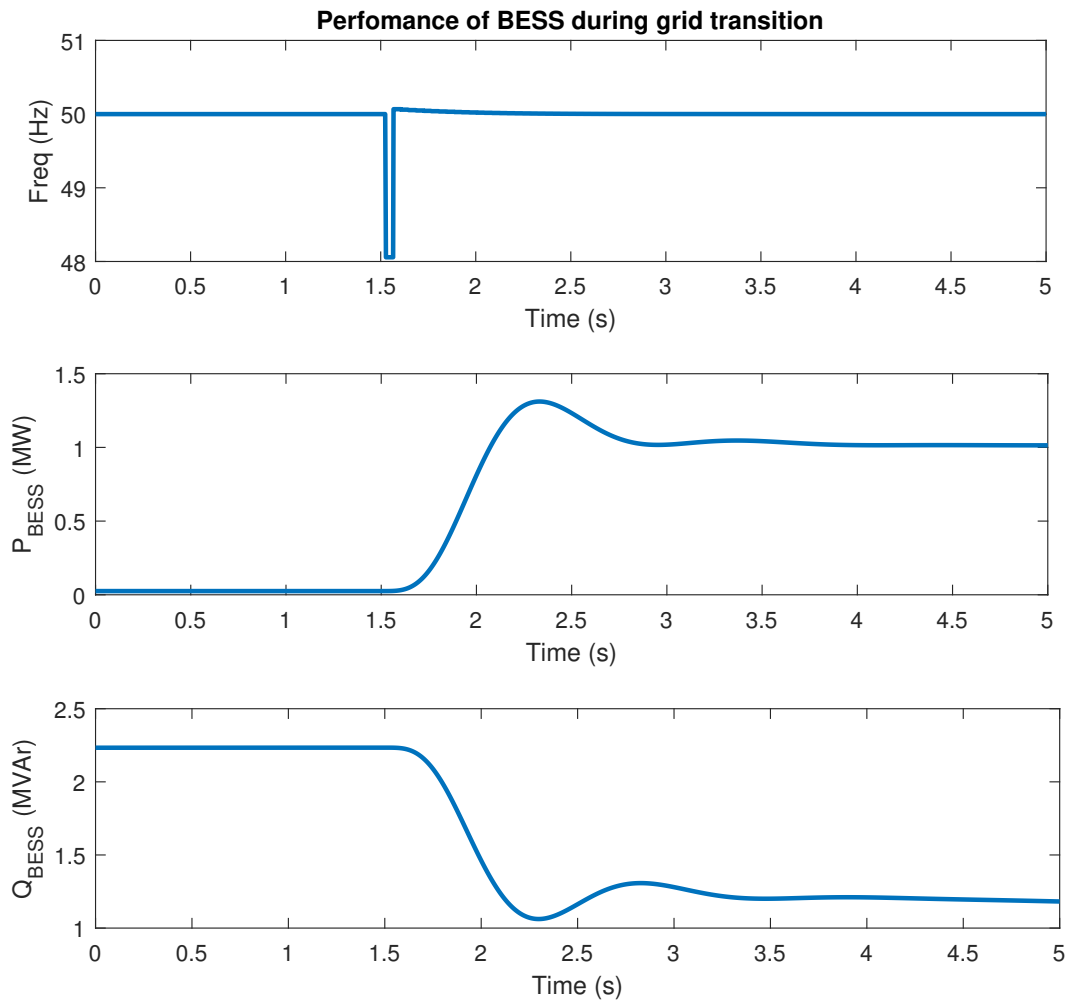


Figure 4.12: Micro-grid - Grid Transition

## 4.10. Voltage control in Micro-grid mode

Figure 4.10 is used to illustrate the ability of the BESS to act as a grid forming source in the case of black start or emergencies. It can be seen that the BESS system can provide active and reactive power to stabilize the grid in this case. In Figure 4.11, a step disturbance of 0.3 MW is introduced at 1.5 s into the micro-grid network without a generator. It can be seen from the figure that the frequency is stabilized quite easily after the disturbance occurs at 1.5 s. The transition (happens at 1.5 s) from a micro grid setup without a generator to that a grid connected mode with a generator is illustrated in Figure 4.12. The BESS is able to provide the necessary active and reactive power support for the generator to come into the system without any system collapse. This is a crucial function and very important in weak grids like the one usually present in ships. The reactive power output of the generator for different scenarios when subjected to a step disturbance of 0.3 MW at 1.5 s is as shown in Figure 4.13 and it can be easily seen that the reactive power output of the generator is higher without the BESS since the generator needs to contribute more reactive power for voltage stability. The system even absorbs a little bit of reactive power in the presence of a BESS. It can also be seen that the power output of the generator is the same for different levels of RES penetration.

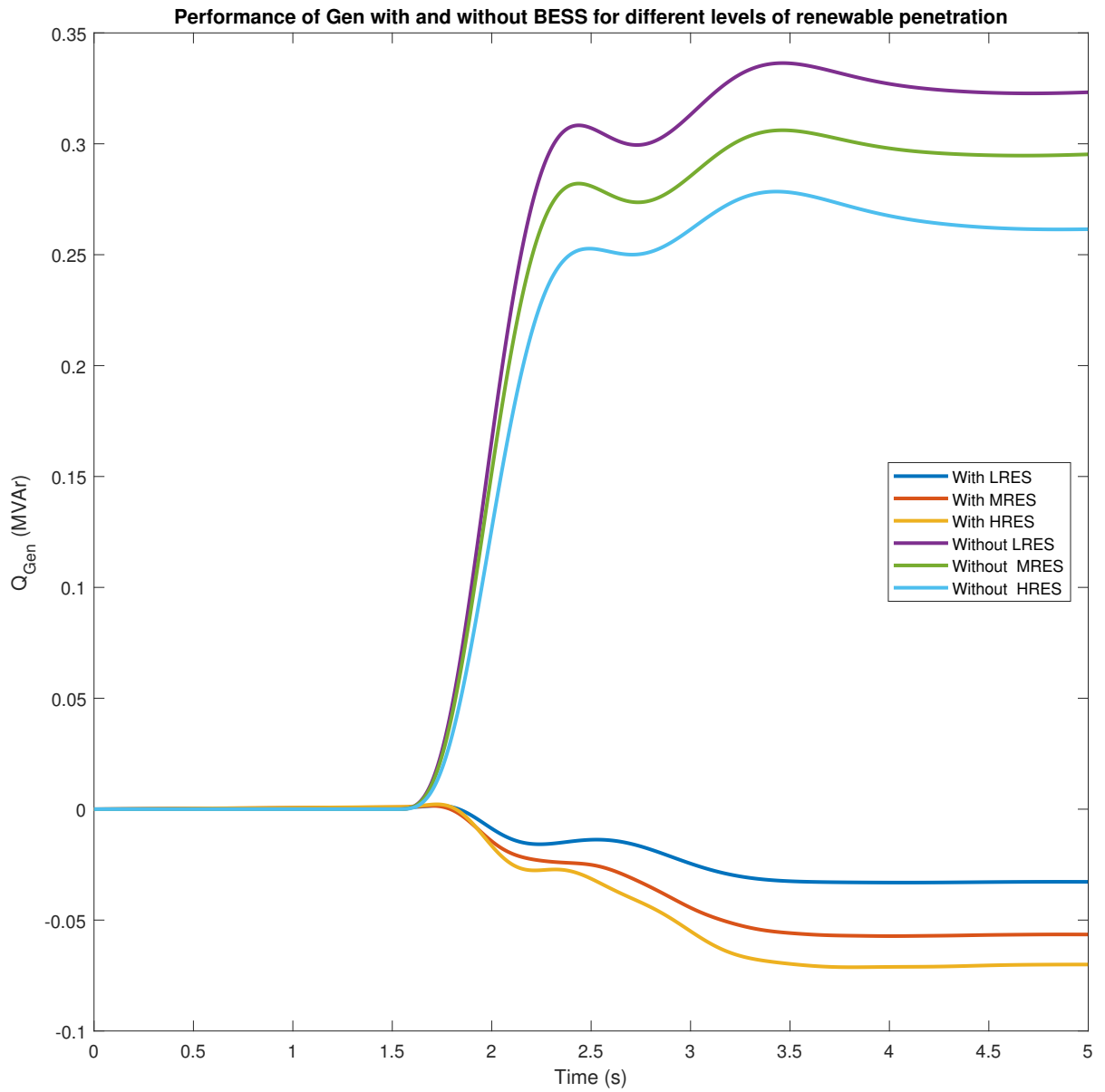


Figure 4.13: Grid connected voltage control with and without BESS - Step Load

## 4.11. Controller Tuning

### 4.11.1. Voltage control

Figure 4.14 shows the reactive power output of the BESS system for different  $K_p$  (proportional gain) values keeping other values constant when subjected to a step disturbance of 0.3 MW at 1.5 s. It was seen that the reactive power output of the BESS increases with decreasing values of  $K_p$  with the highest power output for  $K_p = 0.1675$ . The stability of the voltage is the same for all values of  $K_p$  with the difference negligible (0.01%). For greater BESS contribution during voltage control, the  $K_p$  value needs to be closer to the lower limit of the model which is 0.1675. The observed trend was the same for all levels of RES penetration.

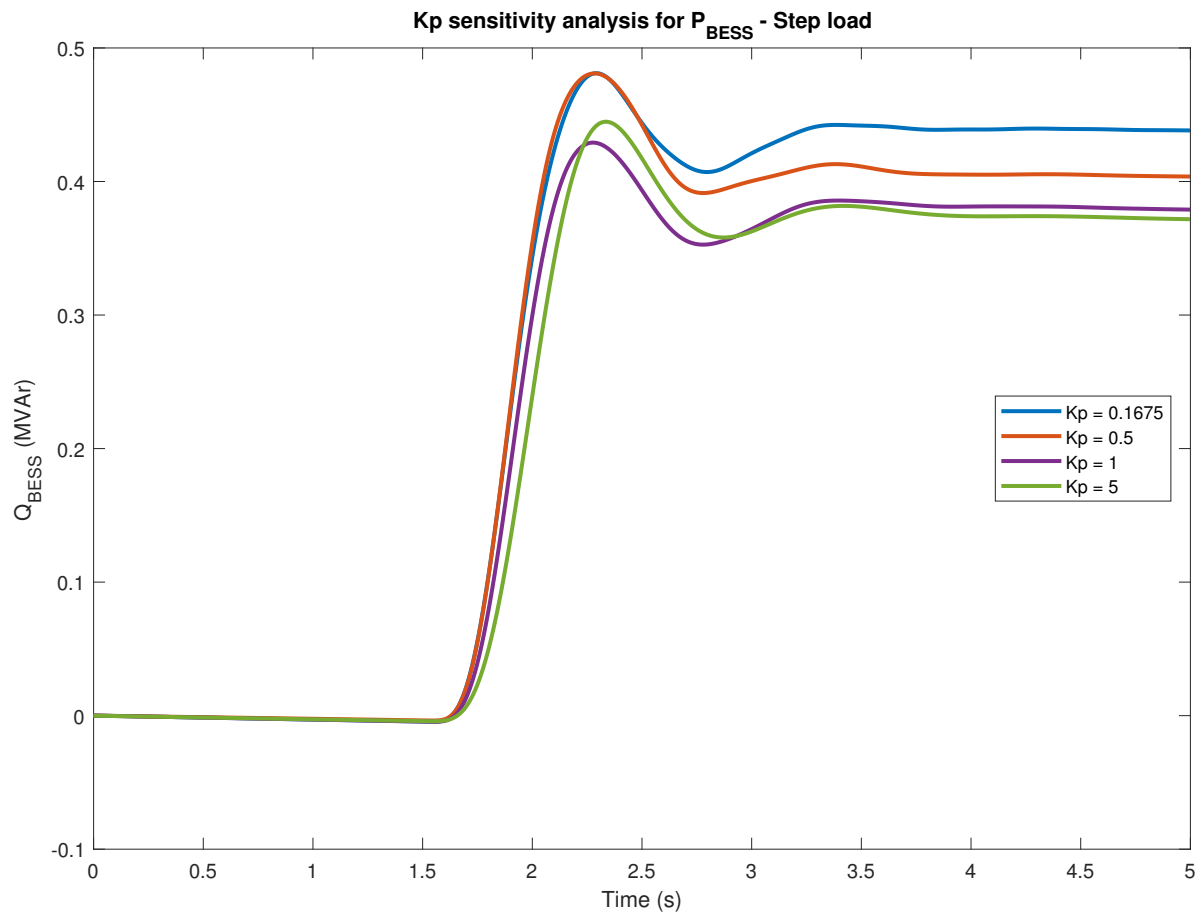


Figure 4.14: Grid connected voltage control Sensitivity Analysis for  $K_p$  - Step Load

The power output of the BESS for different values of  $K_i$  (integral gain) keeping the other parameters constant ( $K_p = 0.1675$ ) when subjected to a step disturbance of 0.3 MW at 1.5 s is as shown in Figure 4.15. It was observed that the power output of the BESS increases with decreasing values of  $K_i$ . The highest reactive power output was observed for  $K_i = 1$ . As with the earlier case, the voltage stability was observed to almost the same for all values of  $K_i$ . For greater BESS contribution for voltage stability, the  $K_i$  value needs to be on the lower side ( $K_i = 1$ ). This was observed for all levels of RES penetration.

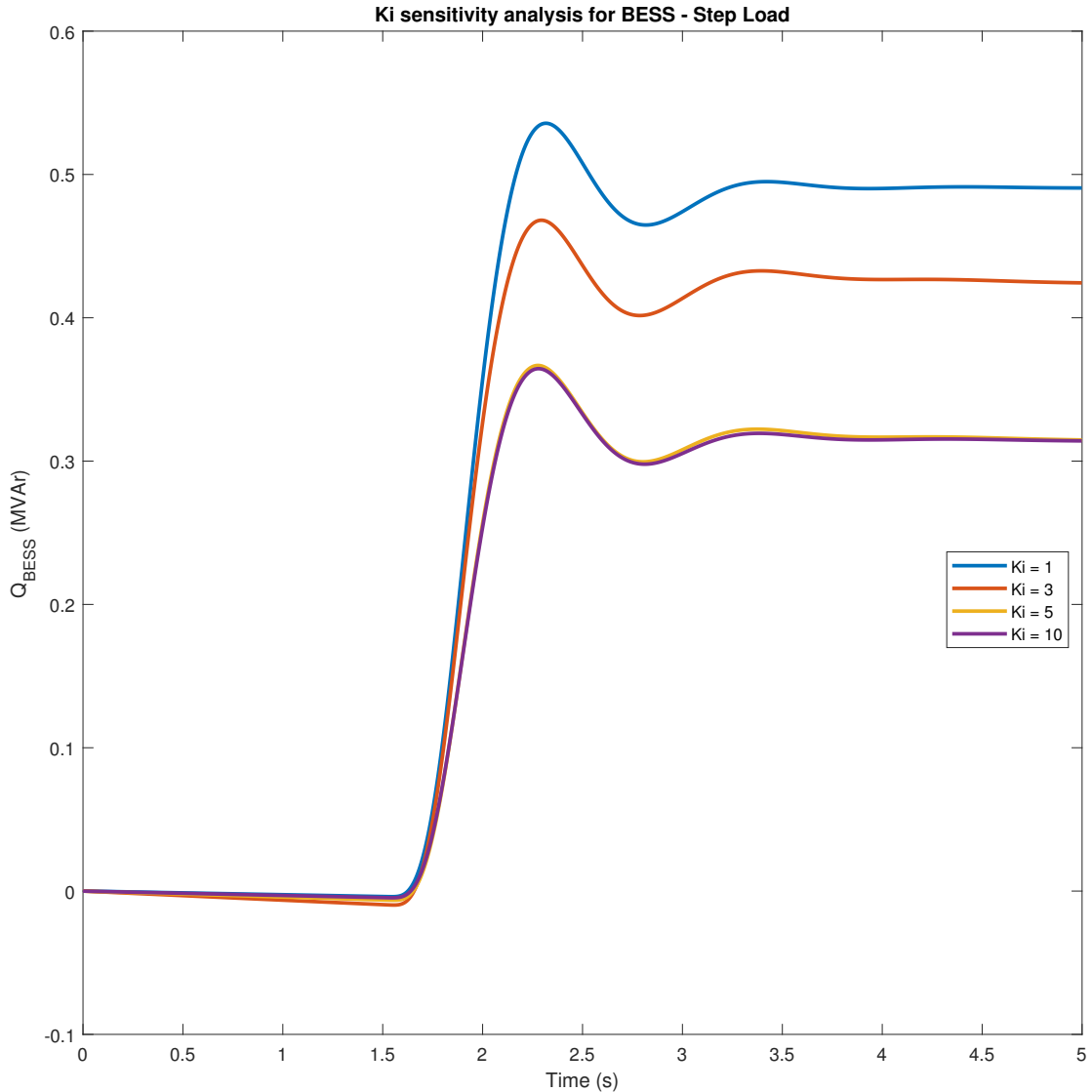


Figure 4.15: Grid connected voltage control Sensitivity Analysis for  $K_i$  - Step Load

### 4.11.2. Primary frequency control and Steady state contribution

Figure 4.16 shows the active power output of the BESS system for different  $K_p$  (proportional gain) values keeping other values of the system constant when subjected to a step disturbance of 0.3 MW at 1.5 s. It was seen that the active power output of the BESS increases with decreasing values of  $K_p$  with the highest power output for  $K_p = 0.025$ . The stability of the frequency is the same for all values of  $K_p$  with the difference negligible (0.01%). For greater BESS contribution, the  $K_p$  value needs to be closer to the lower limit of the model which is 0.025. The observed trend was the same for all levels of RES penetration.

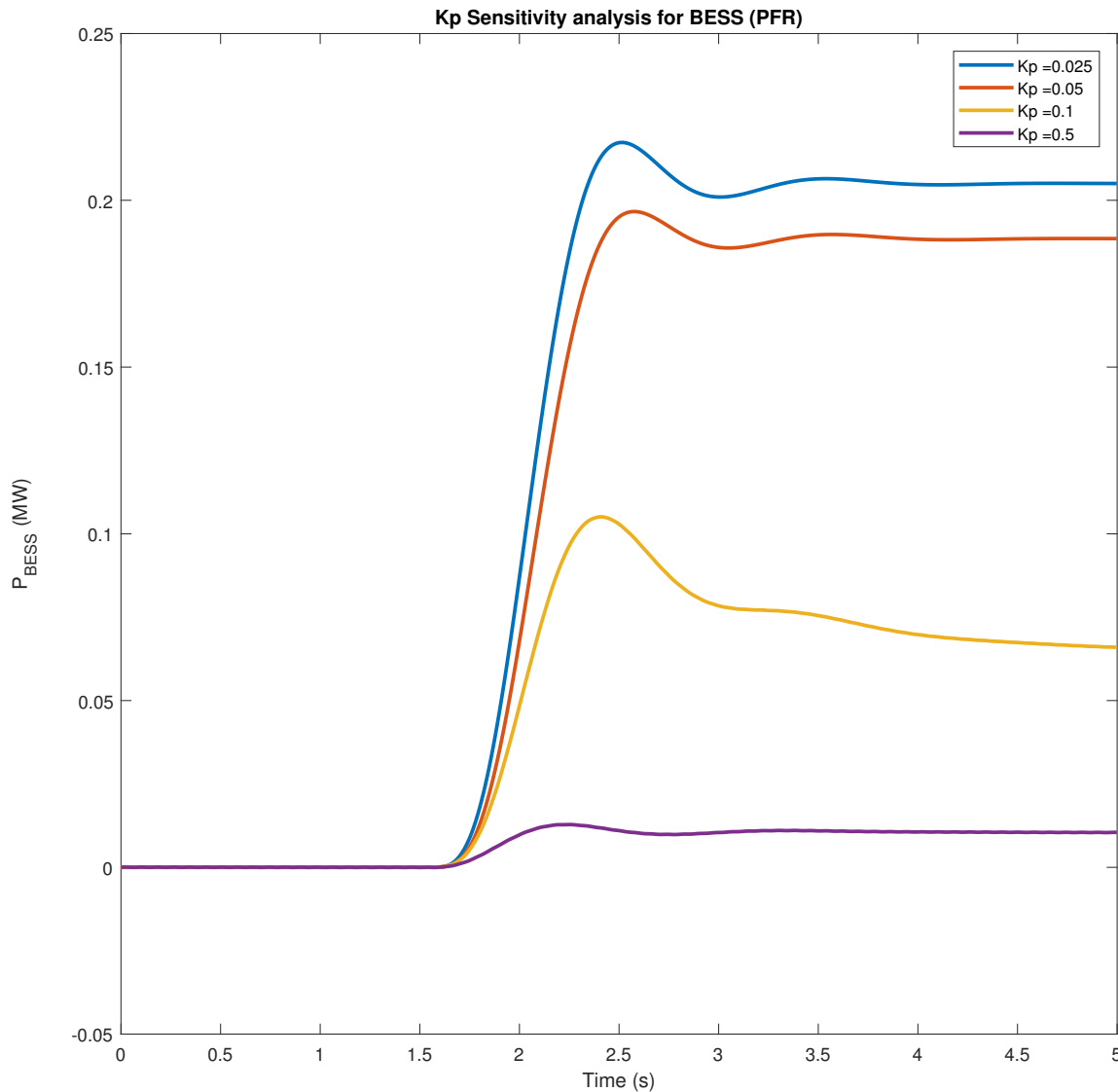


Figure 4.16: Sensitivity analysis for  $K_p$

The power output of the BESS for different values of  $K_i$  (integral gain) keeping the other parameters constant ( $K_p = 0.025$ ) when subjected to a step disturbance of 0.3 MW at 1.5 s is as shown in Figure 4.17. It was observed that the power output of the BESS increases with increasing values of  $K_i$ . The highest power output was observed for  $K_i = 5$ . As with the earlier case, the frequency stability was observed to almost the same for all values of  $K_i$ . For greater BESS contribution for primary frequency response, the  $K_i$  value needs to be on the higher side ( $K_i = 5$ ). This was observed for all levels of RES penetration.

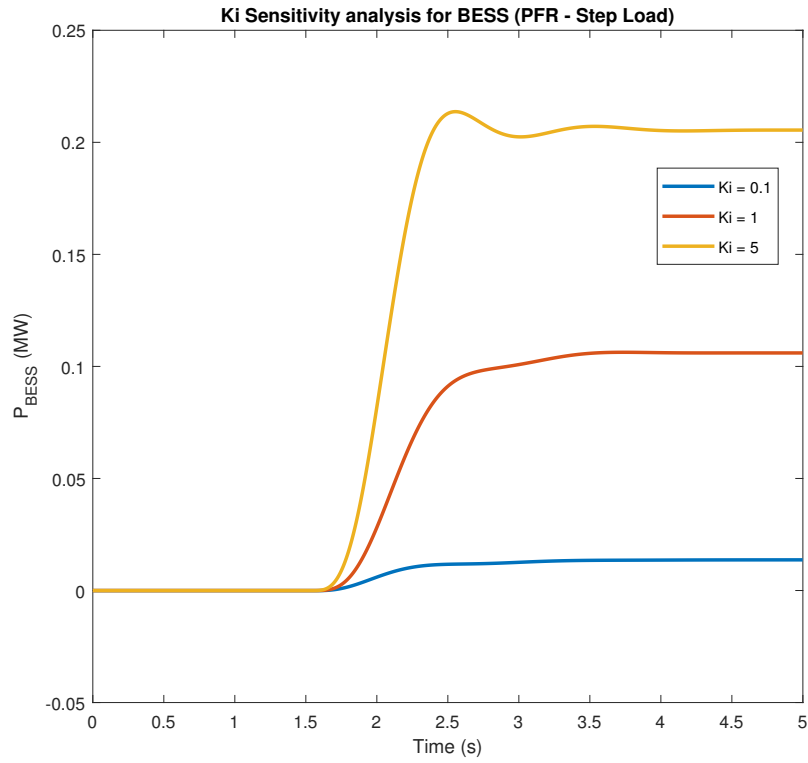
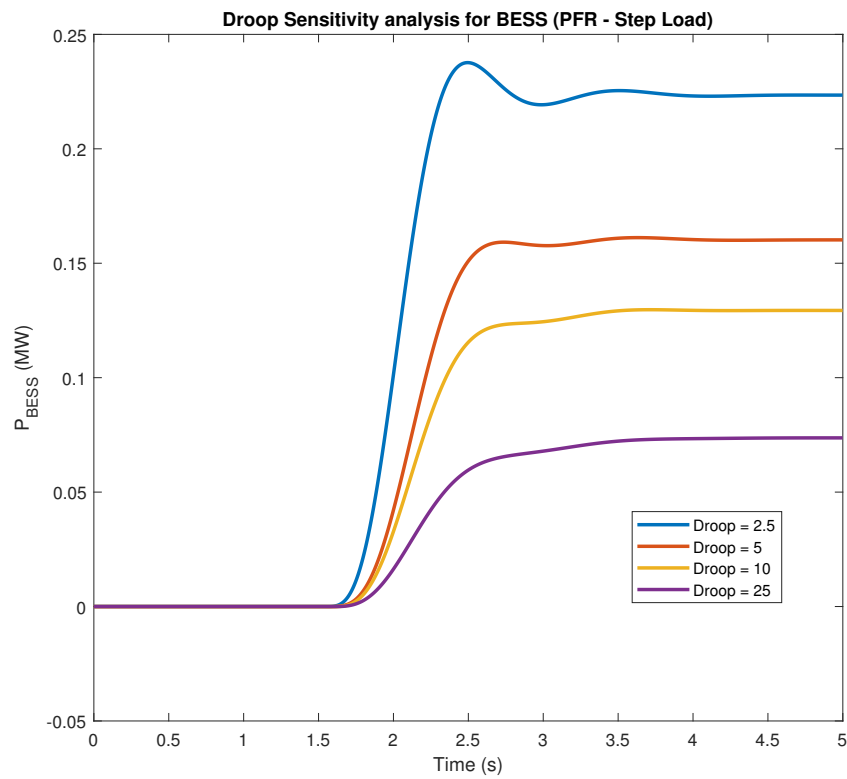
Figure 4.17: Primary Frequency Control Sensitivity Analysis for  $K_i$  - Step Load

Figure 4.18: Primary Frequency Control Sensitivity Analysis for Droop - Step Load

Figure 4.18 shows the BESS power output for different values of droop in the system while keeping other parameters constant when subjected to a step disturbance of 0.3 MW at 1.5 s. As expected, it was observed the system with the lowest droop values contributes the most towards the stability of the system in the event of a step disturbance of 0.3 MW. The generator droop was kept at 2.5% for all the cases and the same trend was observed for different levels of RES penetration



# 5

## Conclusions and Recommendations

### 5.1. Summary of Observations and Key Insights

This section summarizes the content found in chapters 3 & 4. They are as follows:

1. The performance of the generator with and without the BESS for primary frequency control and voltage control was observed and it was clearly seen that the presence of BESS reduces the load of the generator output for both frequency and voltage control.
2. Novel algorithms for frequency control were introduced and a comparison study with the traditional primary frequency control was done. The three algorithms are as follows:
  - Primary Frequency control (Traditional Control Scheme)
  - Peak Shaving (PS) services & Primary frequency control
  - Integrated control for Primary frequency control
3. The application of an integrated control scheme for both frequency and voltage control was illustrated and discussed.
4. The application of BESS for black start and transition from island to grid connected mode was illustrated and discussed.
5. Coordination of multiple BESS with an adaptive droop based on SOC for primary frequency control was illustrated and discussed.
6. The response of the BESS when subjected to time delays in sensing and communication was illustrated and discussed.
7. The controller tuning for primary frequency control contribution of the BESS with respect to various parameters was done and the best fit for performance was found. The parameters are as follows:
  - $K_p$
  - $K_i$
  - Droop
8. The controller tuning for voltage control contribution of the BESS with respect to various parameters was done and the best fit for performance was found. The parameters are as follows:
  - $K_p$
  - $K_i$

## 5.2. Conclusions

It can be seen from the results and discussions presented in chapter 4 that the integrated control scheme is the best in terms of overall stability with the peak shaving control scheme better than the traditional scheme for primary frequency control. The importance of the BESS for providing ancillary services such as frequency and voltage control was also illustrated through the performance of the generator with and without the BESS for different levels of RES penetration. The usefulness of the BESS was also observed when it comes to black starts due to weather conditions or emergencies. It helps in the transition from a black start to a grid connected set up. The use of adaptive droop algorithm to optimize the performance of a portfolio of BES systems in applications such as VPP was illustrated. The robustness of the algorithm was also tested by incorporating a time delay in the system with the results proving the system to be sufficiently robust. The research questions posed in chapter 1 are answered as follows:

**1. What is the effect of the BESS on the overall stability and the performance of generator in the system?**

The effect of the BESS on the system is very clear and obvious from the results observed in Chapter 4. It can be clearly seen that the frequency and voltage stability improves removing any additional stress on the existing sources of generation. This is a crucial feature especially with increasing penetration of RES sources with re-dispatching of resources becoming harder.

**2. How does the BESS perform in the case of black start scenarios?**

The usefulness of BESS is very evident as it provides as a fail safe way for the system to recover in case of emergencies by stabilizing the voltage and frequency of the system before bringing on board the generator.

**3. Does the performance of a VPP improve with the implementation of adaptive SOC based droop?**

The performance of an aggregator like VPP is improved when an adaptive droop based on SOC is applied instead of a traditional droop approach. This helps the VPP provide an optimal power output while maintaining the health of the batteries by ensuring the SOC of any one battery doesn't go too low. The BESS systems needs to reconfigured to limit the power output as the number of BESS systems increases since it leads to frequency volatility if the power is not limited. This is an important consideration that needs to be taken into account before building a VPP portfolio.

**4. Is the performance of an integrated control system better than building individual controls?**

The performance of an integrated control scheme was found to be better than the traditional control scheme used for primary frequency control as explained in chapter 4. As a result, it is recommended to use the integrated control scheme for better performance. Moreover, an integrated control scheme allows the BESS to provide frequency and voltage control at the same time as illustrated in Chapter 4. It can be seen that the settling time for the integrated control is less than the two other control schemes by 1 s.

**5. How robust is the controller when it comes to dealing with time delays in the inverter hardware?**

The robustness of the algorithm was also tested by incorporating a time delay in the system with the results proving the system to be sufficiently robust. The upper limit of the delays is limited to 0.7 s according to [43].

**6. How does the controller perform for different levels of renewable energy penetration in the grid?**

- 1) 30%
- 2) 50%

3) 98%

All the experiments were repeated for different levels of RES penetration and the results were found to be consistent across different levels of RES penetration.

### **5.3. Contributions to IEPG**

The thesis project has developed distribution network models, different control schemes for BESS and tested scenarios, thereby enhancing the understanding of BESS systems and the potential they hold for providing ancillary services and supporting distribution power systems. The contribution to IEPG's ongoing research in this field are outlined as follows:

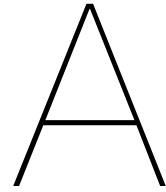
1. Developed and deployed a MV distribution network based on the benchmark model developed by CIGRE Task Force C6.04.02 [52] which can be used for future power system studies on RSCAD by IEPG.
2. Proposed and developed novel control schemes to maximize the capabilities of BESS to deliver ancillary services in a distribution network under different levels of renewable penetration.

### **5.4. Future work**

The role of storage in futuristic distribution grids needs to be explored. Some of them are as follows:

1. There is a need to develop standard test cases for testing in the distribution network which can be used globally for all case studies.
2. It is important to understand and quantify the contribution of each ancillary service component from BESS if it is supplying more than one at the same time.
3. Communication from sensors to BESS control is an important part of the system and more research needs to be done to test the robustness of the system in case communication is shaky and not fully accurate.





# User Manual

## A.1. Objective

The BESS system in real life is represented by a BESS model in RSCAD. The model has two distinct parts, the basic model comprising the power electronics part and the second one being the controller logic which facilitates the usage of BESS for providing ancillary services in a distribution system. The purpose of the Appendix is to help the user better understand the key parts of the the model, run the simulation and modify model parameters. This model can be run on a PC which has RSCAD 5.0 installed and an IP (Internet Protocol) connection to an RTDS simulator.

## A.2. Procedure

### A.2.1. LOADING THE DRAFT FILE

This section helps the user understand the procedure for loading of the Draft file. The steps are as follows:

1. Launch the RSCAD software
2. Launch RSCAD's Draft module from the file manager window by double clicking on the relevant file with ".dft" extension. The model will be as shown in Figure A.1
3. Proceed to select the rack and compile the circuit.

### A.2.2. Power calculation block

The electrical parameters such as power outputs and voltages of the different blocks are measured using various meters as shown in Figure A.2

### A.2.3. Runtime

The Runtime module is a companion to the draft module which aids in running the necessary simulations. A snapshot of the Runtime window is shown in Figure A.3. The different sources and loads can be controlled using the switches and sliders in the Runtime window. All the relevant parameters can also be conveniently monitored using plotters.

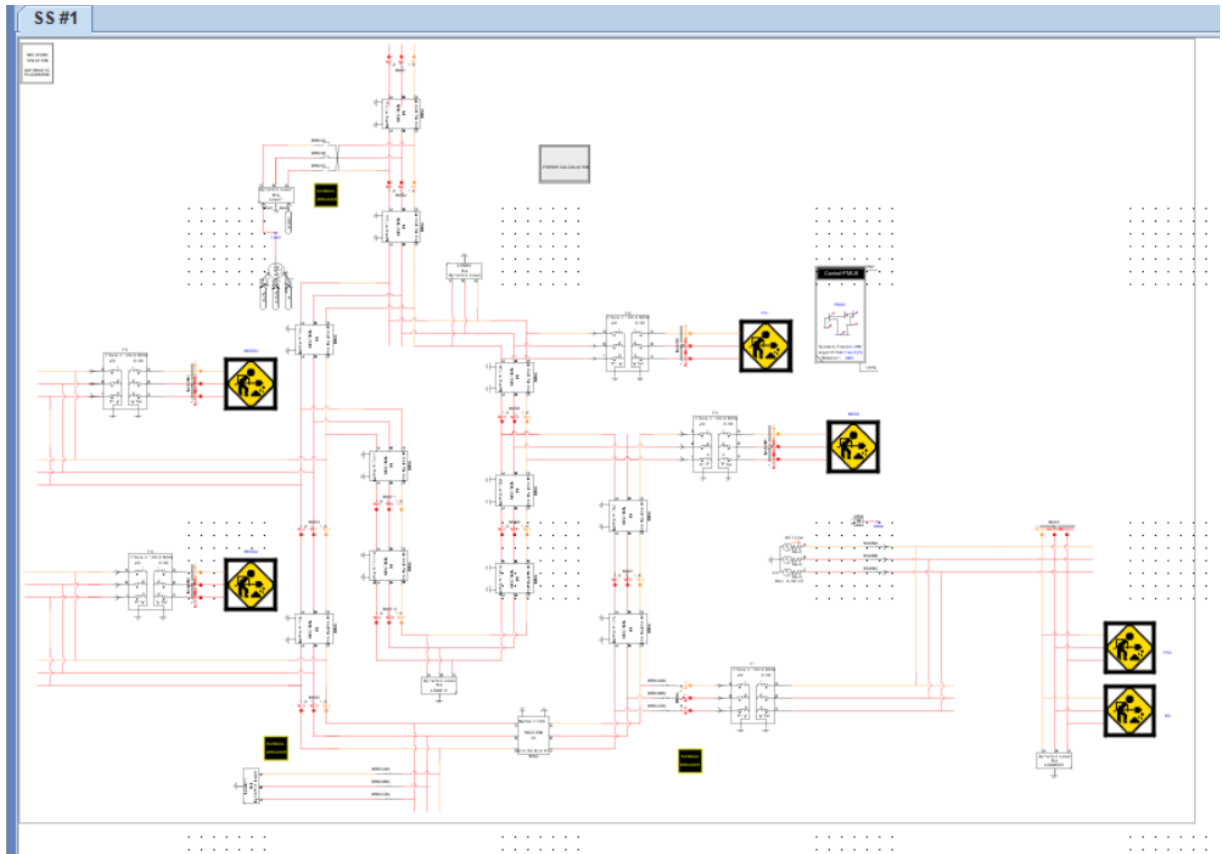


Figure A.1: Benchmark network on RSCAD

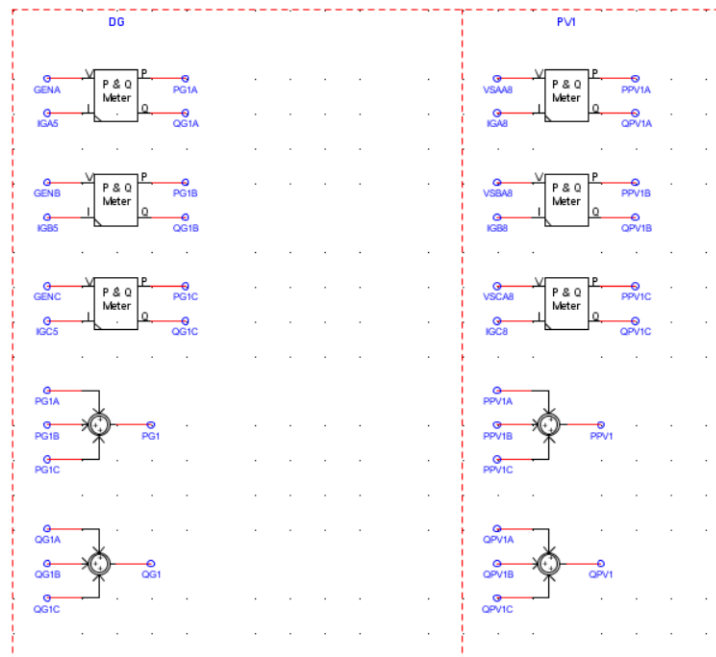


Figure A.2: Benchmark network on RSCAD

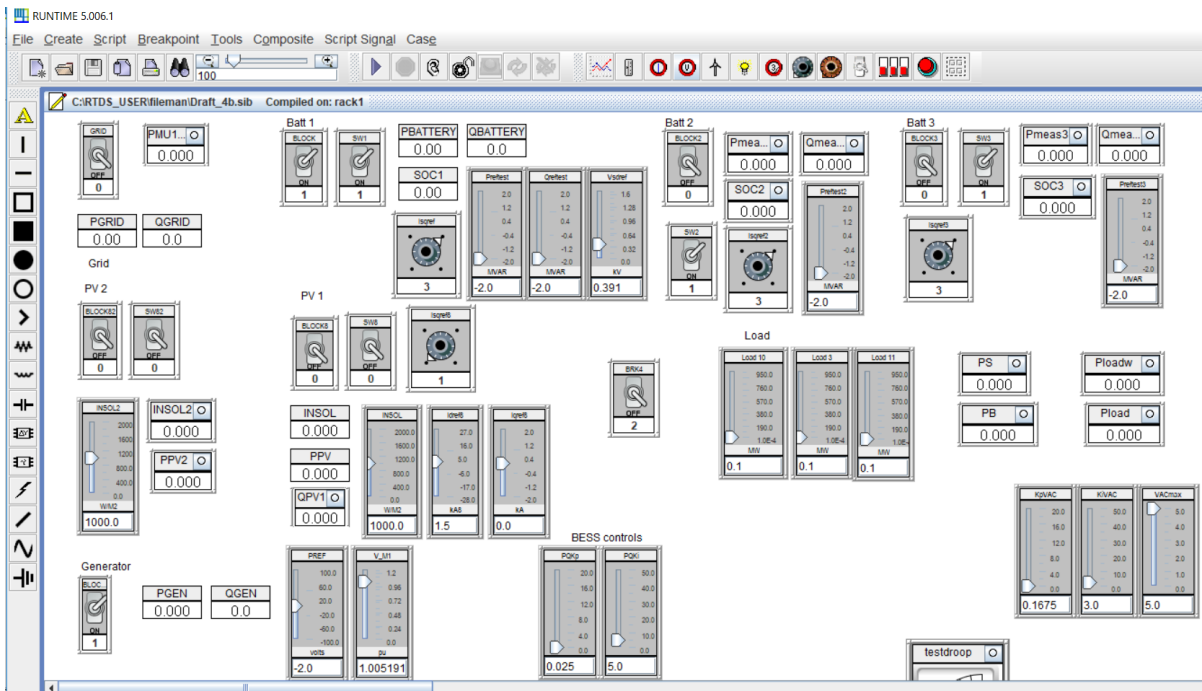


Figure A.3: Benchmark network on RSCAD



# B

## RTDS: Hardware and Software Introduction

RTDS is the state of the art integrated computing system used to study and analyze Electromagnetic Transient (EMT) phenomenon occurring in power systems. The main advantage of RTDS is its ability to perform simulations of power system models at a time scale equal to that of real time operation of the grid. As a result, it is one of the widely used software to validate a piece of hardware employing a control system algorithm to be used in the electrical grid. It provides a safe and controlled environment to perform tests using the HIL (Hardware in loop) method. This would not be possible with most other modelling software since only RTDS mimics the operation of a real live grid. Some of the common areas of testing include pre-testing of new protection and control algorithms, contingency and reliability analysis, etc. The IEPG department in TU Delft has a RTDS simulator as shown in Figure B.1 .The RTDS system in TU Delft consists of 8 racks used simultaneously for various research projects within the department.



Figure B.1: A typical RTDS hardware setup

## B.1. RTDS Hardware

The high speed computing required for real time simulations is achieved by using high speed DSP (Digital Signal Processor) chips and RISC (Reduced Instruction Set Computer). Each rack in the RTDS system is a 19 inch housing unit which has the processor, I/O cards and other units mounted in it as per the functionality. It is powered using an external supply located at the bottom. Some of the hardware components in RTDS are explained below. They are as follows:

- **GTWIF: Giga Transceiver Workstation Interface Card** : GTWIF is responsible for establishing and maintaining the communication between the processing hardware and workstation running RSCAD. The connection is established via an Ethernet based LAN system and it performs the crucial task of transferring data to and fro from the processor unit and the workstation running RSCAD.



Figure B.2: RTDS GTWIF card

- **Global Bus Hub** : The global bus hub (GBH) interface unit as shown in Figure B.3 is necessary when more than 2 racks are used to simulate the RTDS model on RSCAD. This is achieved by interlinking each rack of the RTDS unit to the GBH via a fibre optic cable available on the rack's GTWIF card.



Figure B.3: The RTDS Global Bus Hub

- **PB5: Processor Cards** : The PB5 processor unit is as shown in Figure B.4 and contains two Freescale MC74448 RISC processors each operating at 1.7 GHz. It is the main computational unit in RTDS capable of performing complex computations that can be used for solving network solutions.

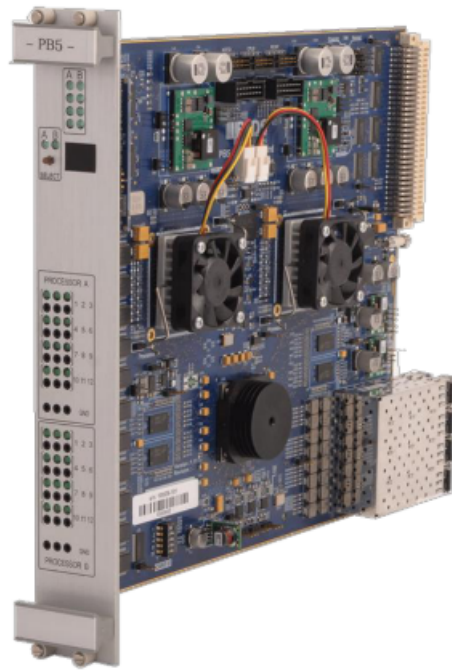


Figure B.4: The RTDS PB5 processor card

- **NOVACORE:** The NOVACORE processor as shown in Figure B.5 is the state of the computing device from RTDS and features IBM's POWER8 processor, containing 10 powerful cores running at 3.5 GHz. It is reverse compatible with the existing RTDS hardware components and each NOVACOR chassis has 2-3 times the simulation capacity of a fully loaded PB5 processor.

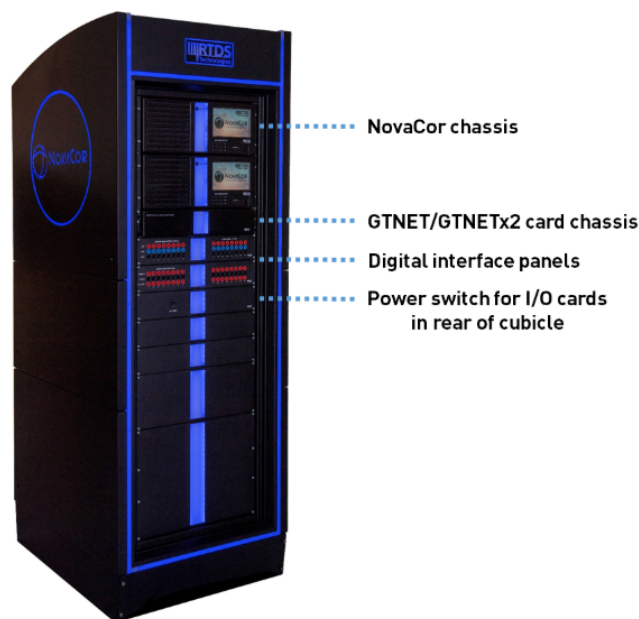


Figure B.5: The RTDS NOVACOR

- GIGA-Transceiver Input/Output (GTIO) cards : GTIO are the interface units which transfer data between the RTDS and other external units. It is driven by the Giga-Transceiver (GT) optical ports located on the PB5 cards. There are different types of GTIO cards and can also be daisy chained if necessary. They are as follows:
  1. GTDI (For digital input)
  2. GTDO (For digital output)
  3. GTAI (For analog input)
  4. GTA0 (For analog output)

## B.2. RTDS Software Interface

The RTDS hardware is accessed and utilized through a proprietary software named RSCAD. The interface on RSCAD enables the user to model, run and analyze different simulation cases with the help of different modules. The different modules are as follows:

- File Manager : It is the section of the software which is used to launch the other modules of the software as shown in Figure B.6. The various draft and simulation files are organized according to projects and users in the file manager.

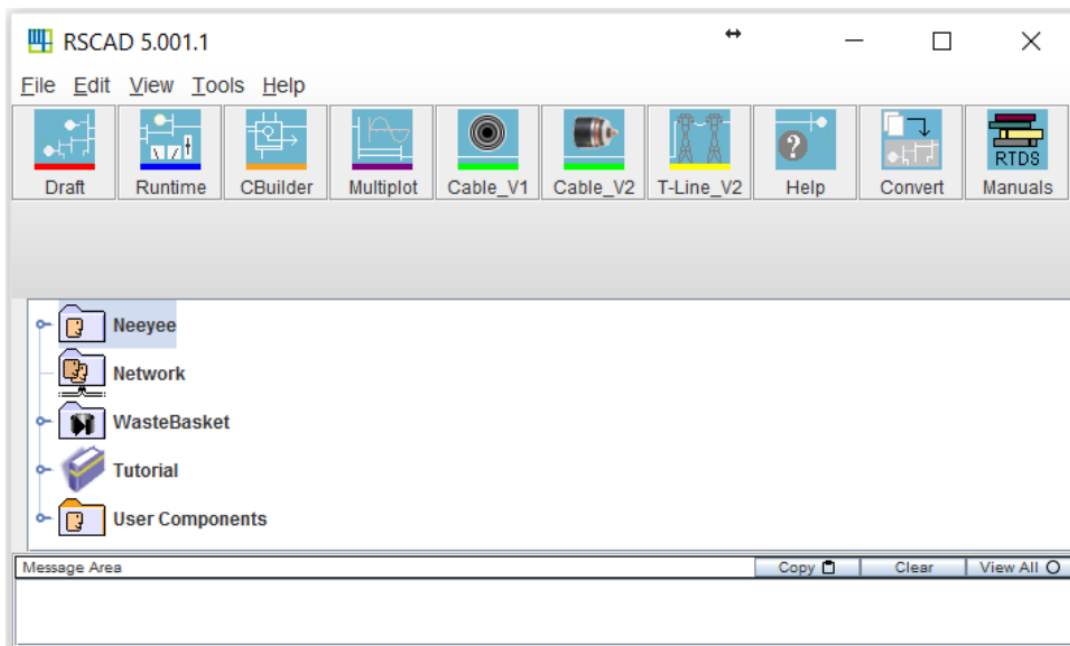


Figure B.6: RTDS File Manager Module

- Draft : The draft module enables the user to graphically create the power system circuit that is required to be simulated . This is done with the library of components available as a part of the draft module as shown in Figure B.7. The user can choose to assemble the circuit in either 3 phase or a single line format which is a unique feature of RSCAD. Once the intended circuit is complete, the model is checked for compilation errors and synced with the RTDS hardware ready for simulation.
- RTDS Library: The RTDS library is part of the Draft module. It includes power system, control system, protection and automation, and small time-step components libraries which can be used to build the desired simulation circuit. A sample of the power system of the control library is shown in Figure B.8.

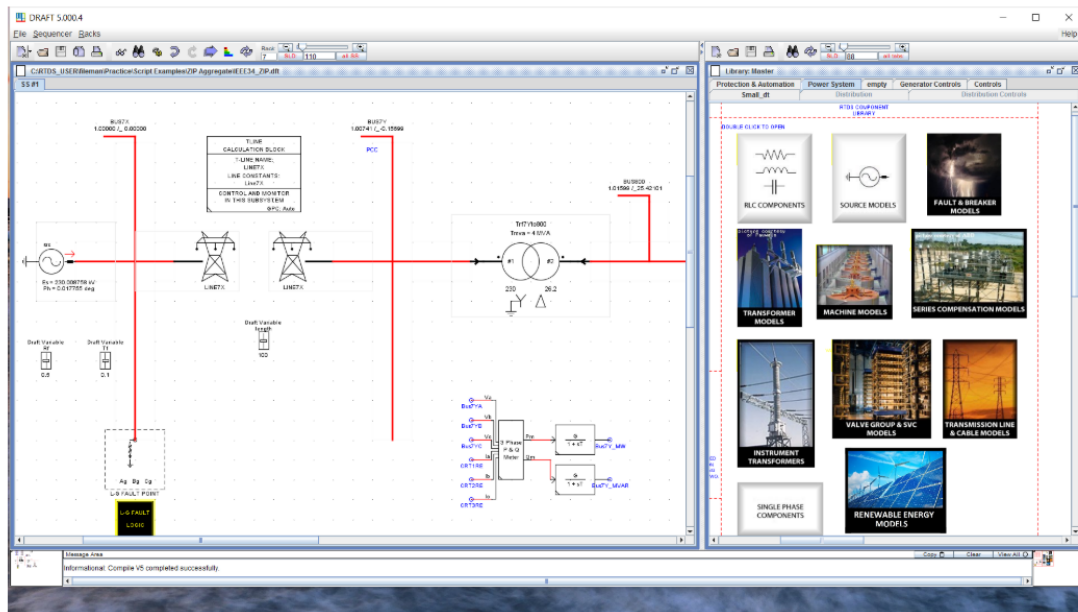
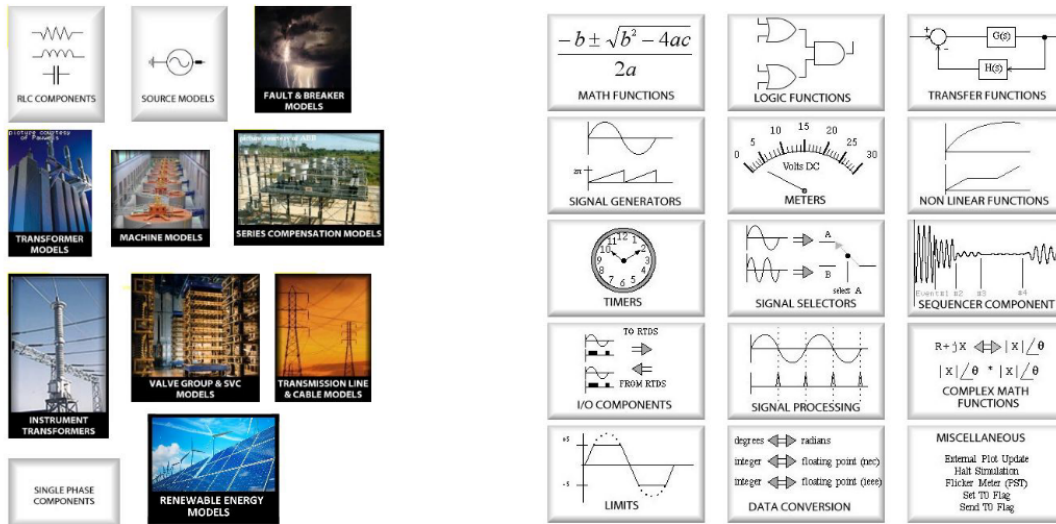


Figure B.7: RTDS Draft Module



(a) Power system library

(b) Control system library

Figure B.8: RTDS Power System and Control Library

- **RunTime** : This is the interface model which enables the user to run simulations on the RTDS hardware. Once the module is simulated on RunTime, the power system model is constantly being simulated on the RTDS hardware. This is particularly useful if the user wants to observe real time responses to disturbances and user initiated events. The user can customize and adjust parameters through components like sliders, switches, buttons, dials, etc. while the simulation is in progress as shown in Figure B.9. The results on the RunTime module can be exported to MS Excel or Matlab for further analysis and processing if necessary.

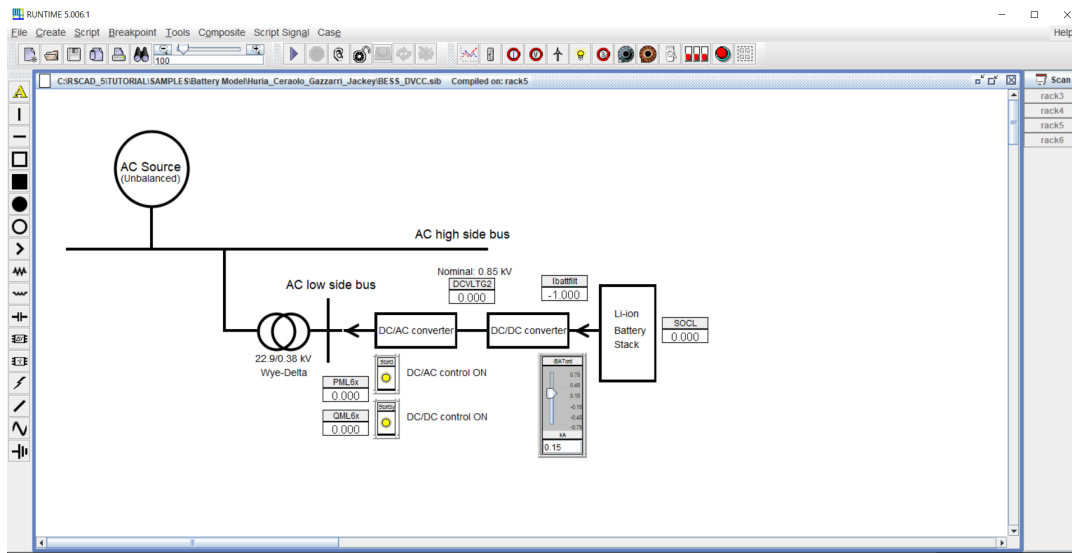


Figure B.9: RTDS RunTime module

- **TLine** : Transmission lines can be modelled in a detailed manner in RSCAD as this is necessary for EMT studies in transmission networks. This is done by creating a user defined module on TLine as shown in Figure B.10. It is generally modelled in RSCAD using travelling wave algorithms. If it is less than 15 km, it is modelled as a RLC PI-circuit. The data defined in the TLine module can be called into the draft module by defining the transmission tower components in the library.

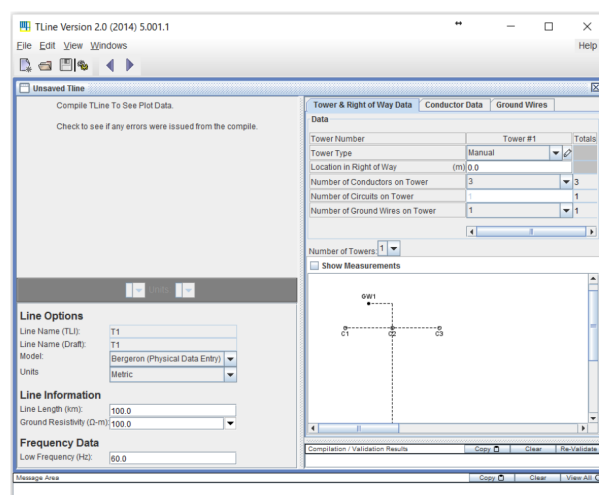


Figure B.10: RTDS TLine module

- Cable : Similar to a transmission line, cables can be modelled comprehensively in RSCAD. It also needs to be called into the draft module using specific cable components in the library.

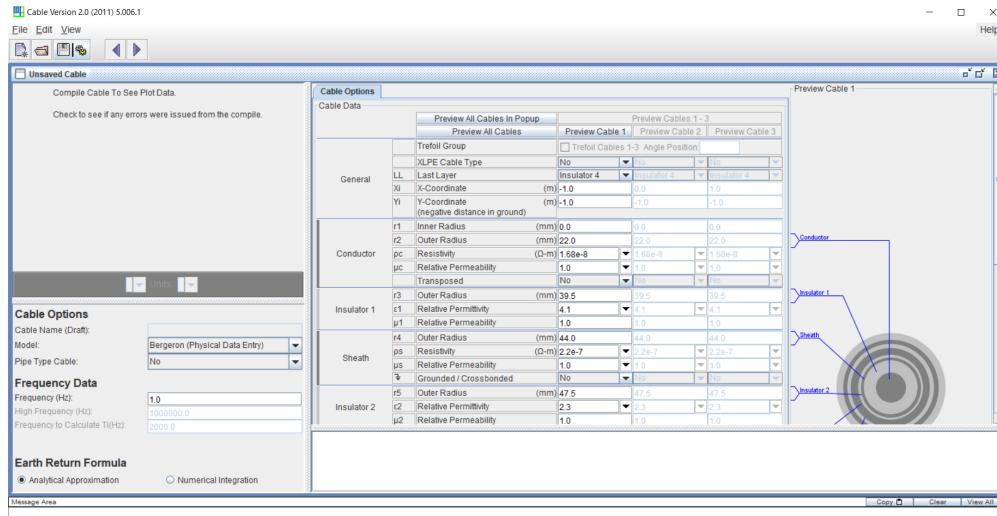


Figure B.11: RTDS Cable module

- Multiplot : This module is used for post processing, analysis and publishing of results that are captured in the RunTime module. Data can also exported to Excel or Matlab from this module.
- Convert : The convert module allows conversion of simulation files that were initially built in another software like PSS/E and PSCAD to RSCAD. It allows the user to easily simulate in real time models that were developed in other established software.
- CBuilder : The Cbuilder module allows the user to create components which are not readily available in the RTDS library as shown in Figure B.12 . This provides the user an extended canvas to customize the circuit according to the needs of the project.

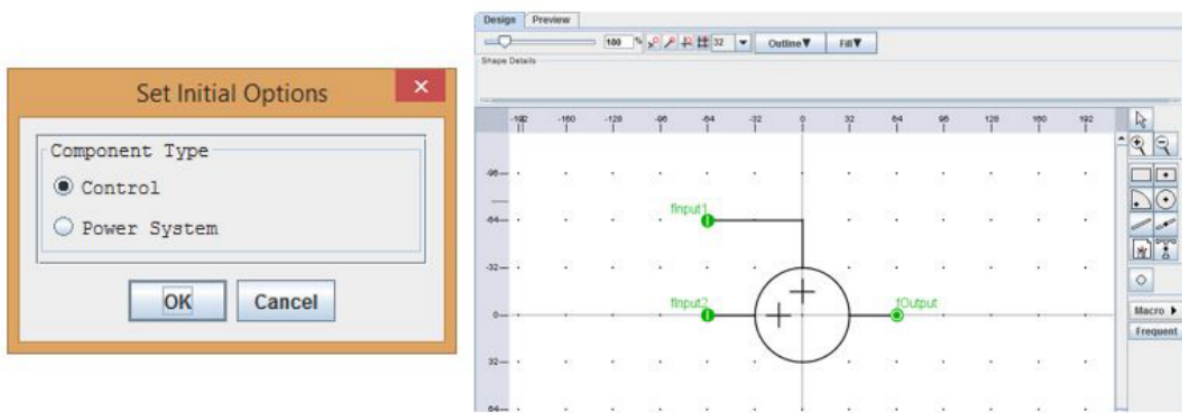
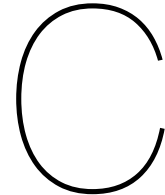


Figure B.12: RTDS Cbuilder module

### B.3. Software Implementation in RTDS

For the user to fully utilize the functionality of the RTDS system, both the software and the hardware need to be set up and linked through a LAN communication. The different power system component models are precisely modelled using the RSCAD software suite while the RTDS hardware employs the nodal analysis technique based on Dommel's solution algorithm to provide network solutions. The subsequent sections provide more information into some aspects of the simulation procedure in RTDS

- **Nodes:** A node in RTDS is defined as the point of interconnection between two power system components in the draft module. The maximum number of nodes that can be accommodated per network solution in a PB5 processor card is 90 single phase nodes or 30 three phase nodes. Moreover, a PB5 processor card can handle up to two networks doubling the capacity of nodes available (i.e.  $2 \times 90$ )
- **Simulation Time Step :** The computation for the different values in an electrical power system is done for integral values of time. The parameters such as node voltage and branch currents are dependent on the calculated values from the previous time steps. Selection of an appropriate time step is important to replicate real grid networks. The RTDS hardware solves the required equations for the state values within the user defined time step. It has two range of time steps in the range of 50 and 2.5 microseconds for normal and high frequency simulation studies.
- **Subsystems:** Subsystems is a well known device concept employed in RTDS and other EMT software. The circuit which is placed inside a subsystem is decoupled from the rest of the power system circuit and be solved independently as an isolated mathematical model. This can be used to split a complex model into smaller subsystems to solve them separately, reducing computational time.



# RSCAD control schemes

## C.0.1. BESS Control Block

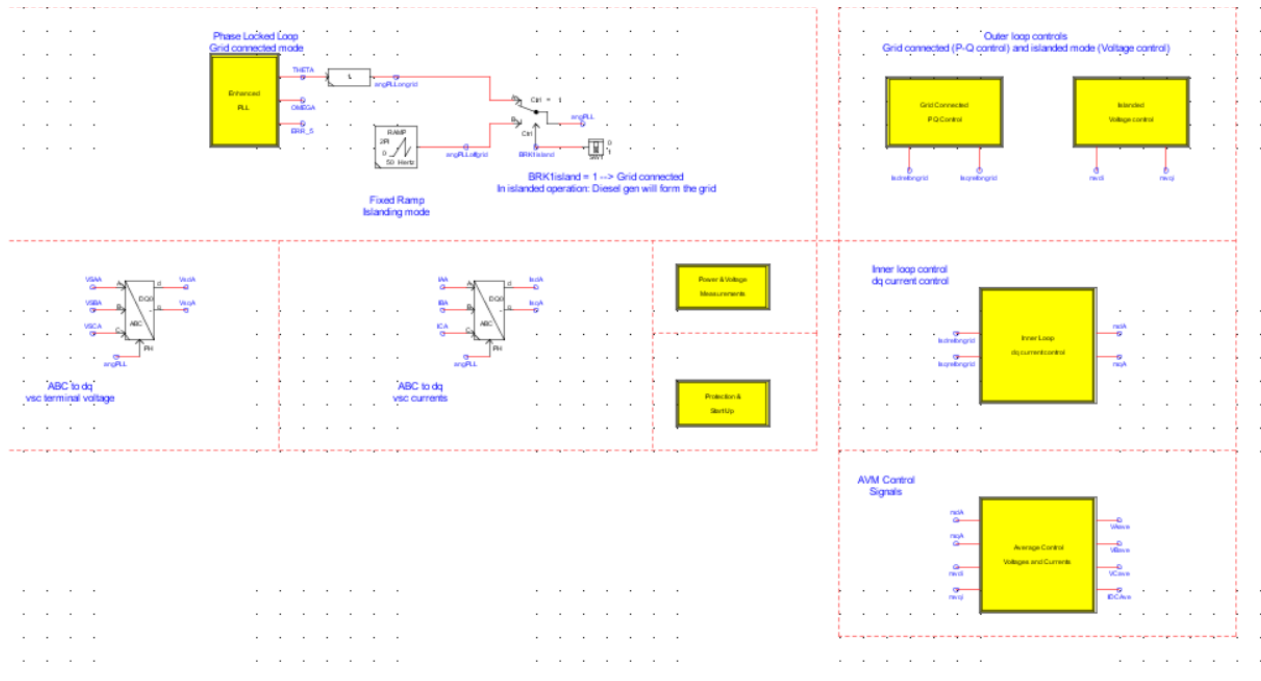


Figure C.1: BESS control block

### C.0.2. PV Control Block

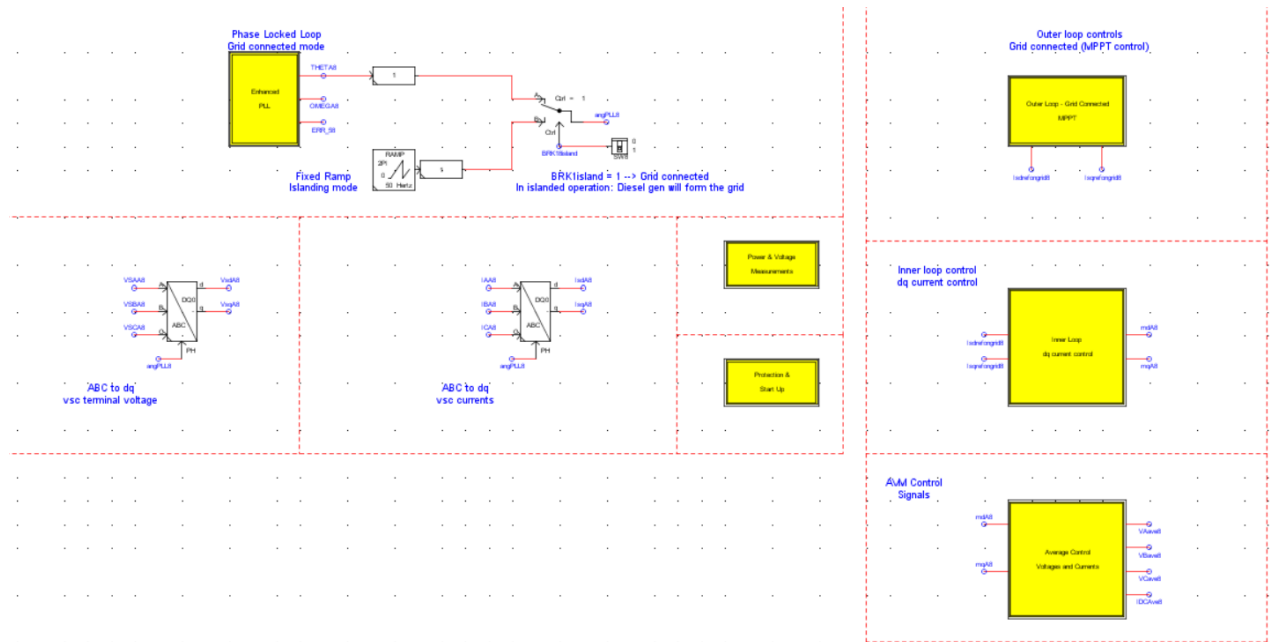


Figure C.2: PV control block

### C.0.3. Primary Frequency Control

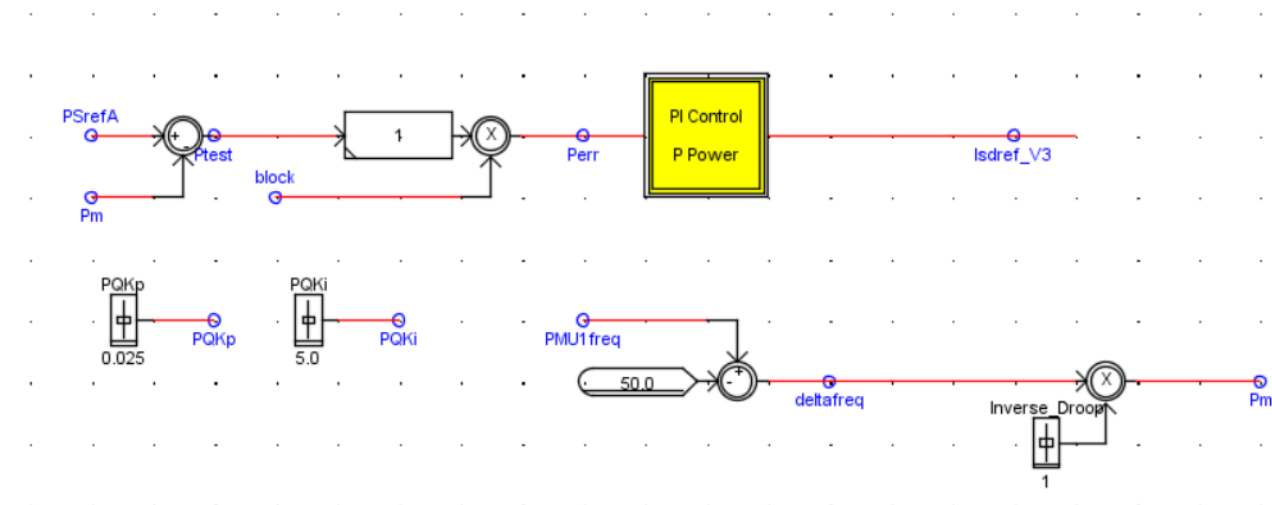


Figure C.3: Frequency control

### C.0.4. Frequency & Peak Shaving Control

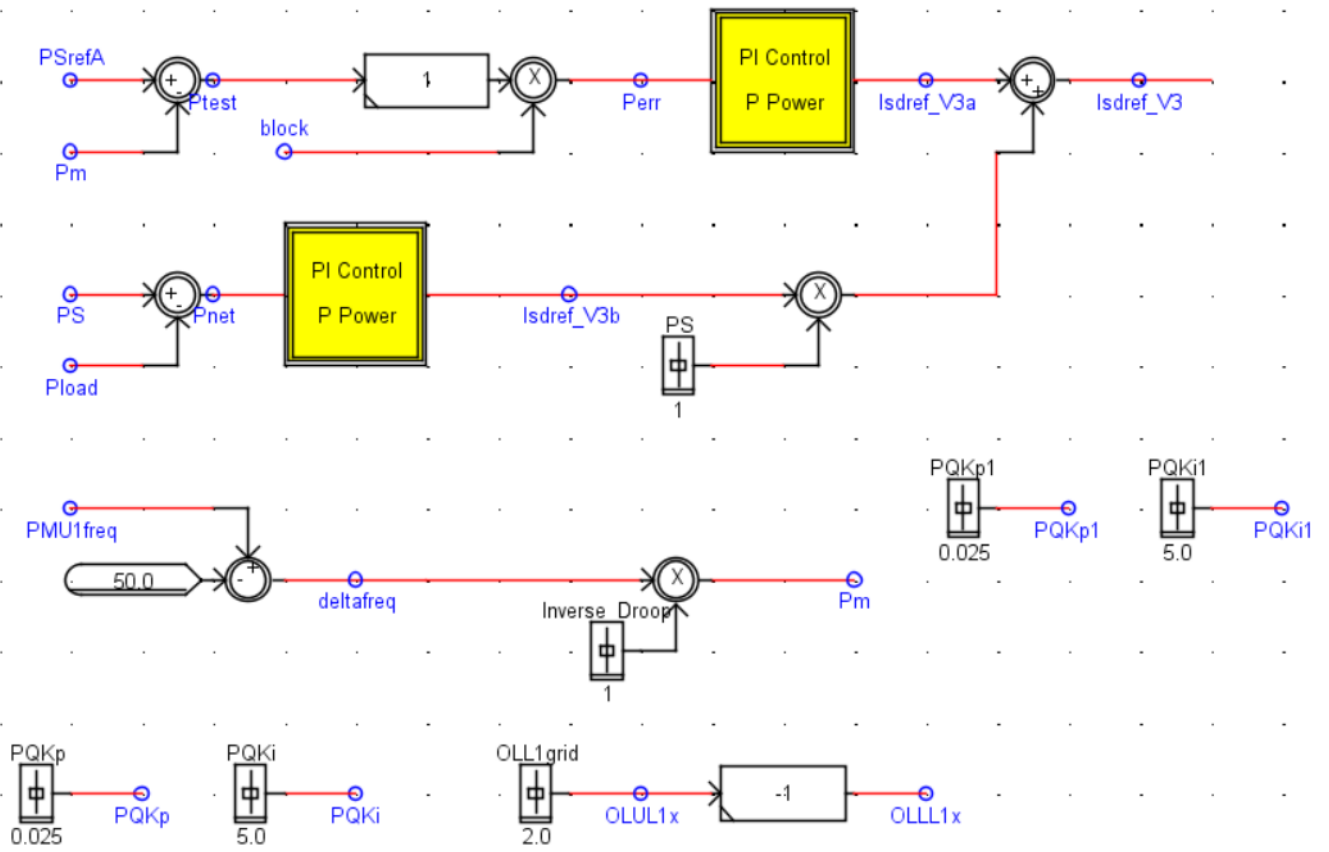


Figure C.4: Frequency & Peak-shaving control

### C.0.5. Integrated Control

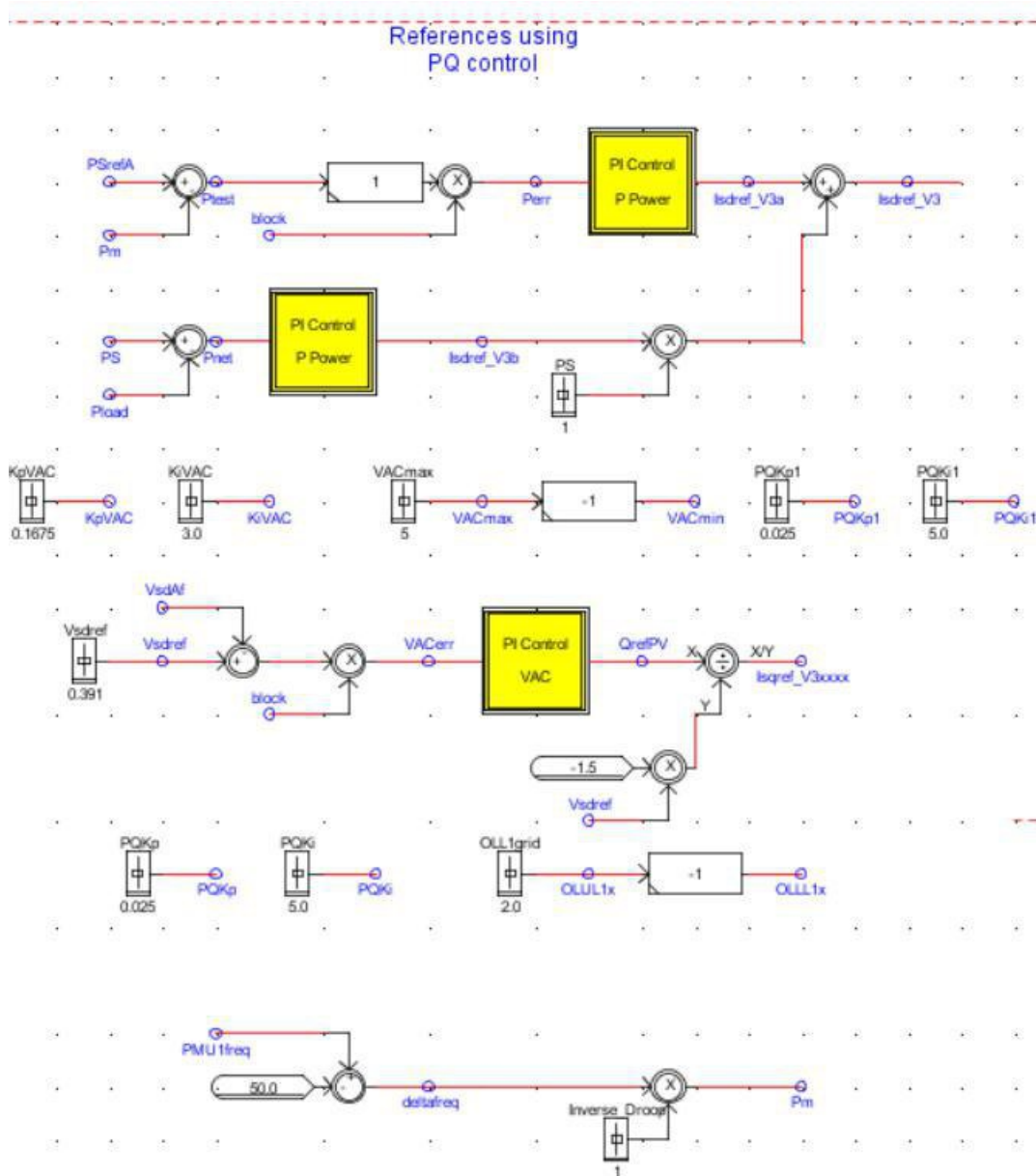


Figure C.5: Integrated control

### C.0.6. Integrated Control with Multiple BESS

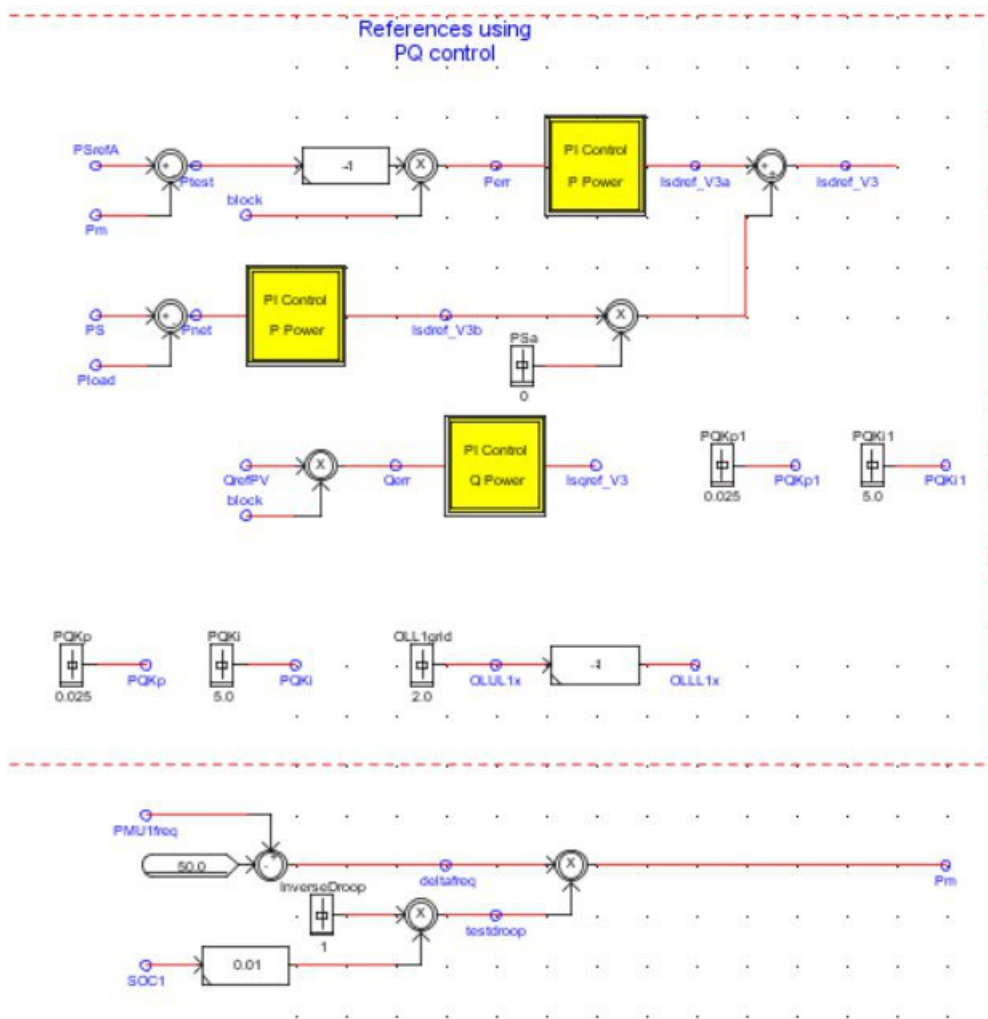


Figure C.6: Integrated control with multiple BESS

### C.0.7. Integrated Control with Time delay

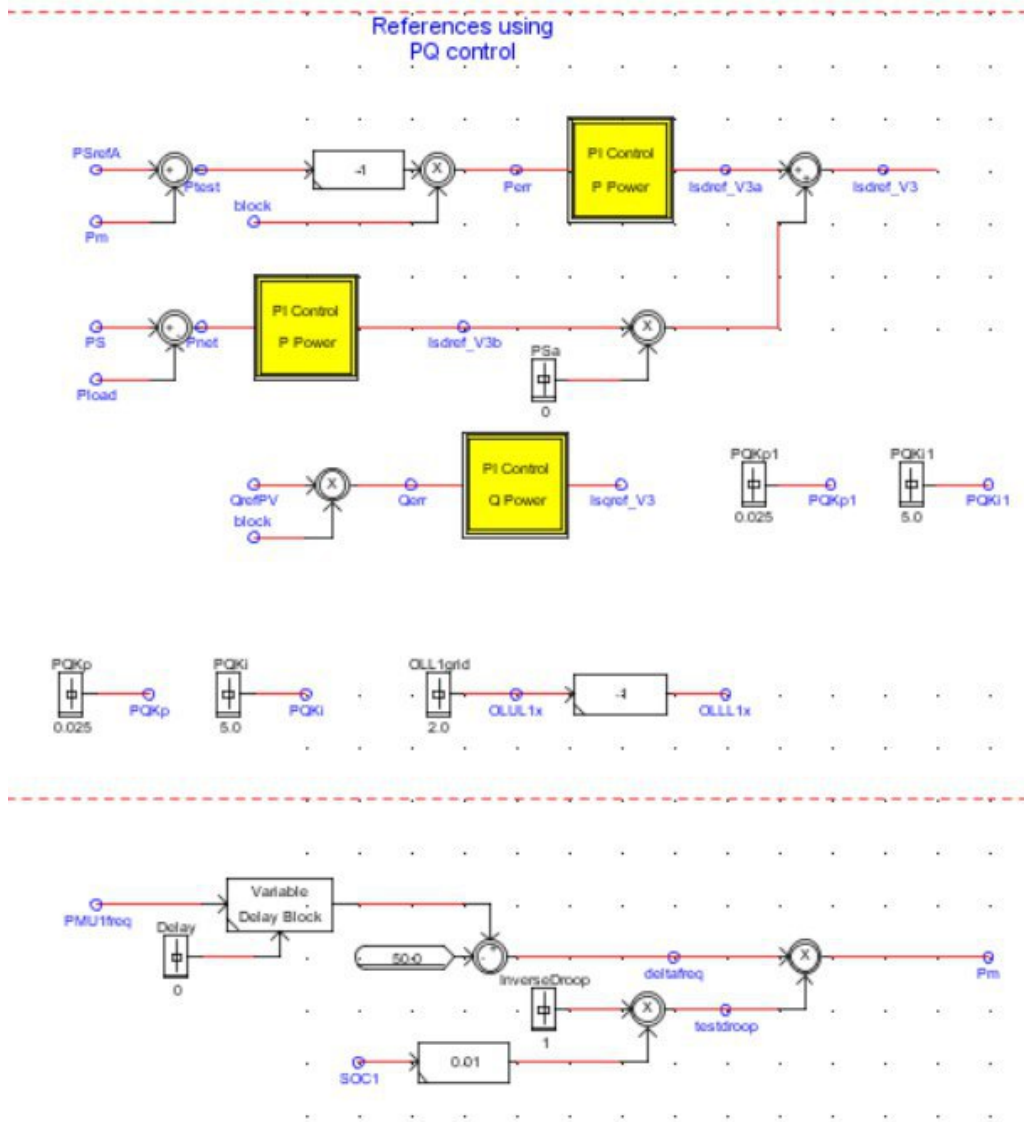


Figure C.7: Integrated control with time delay

## C.0.8. Microgrid Voltage control

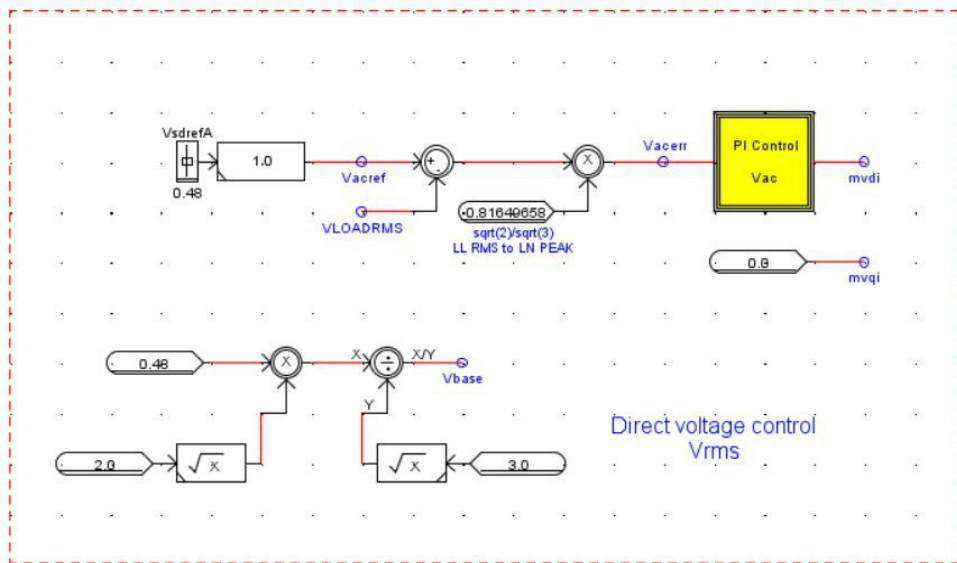


Figure C.8: Micro-grid voltage control

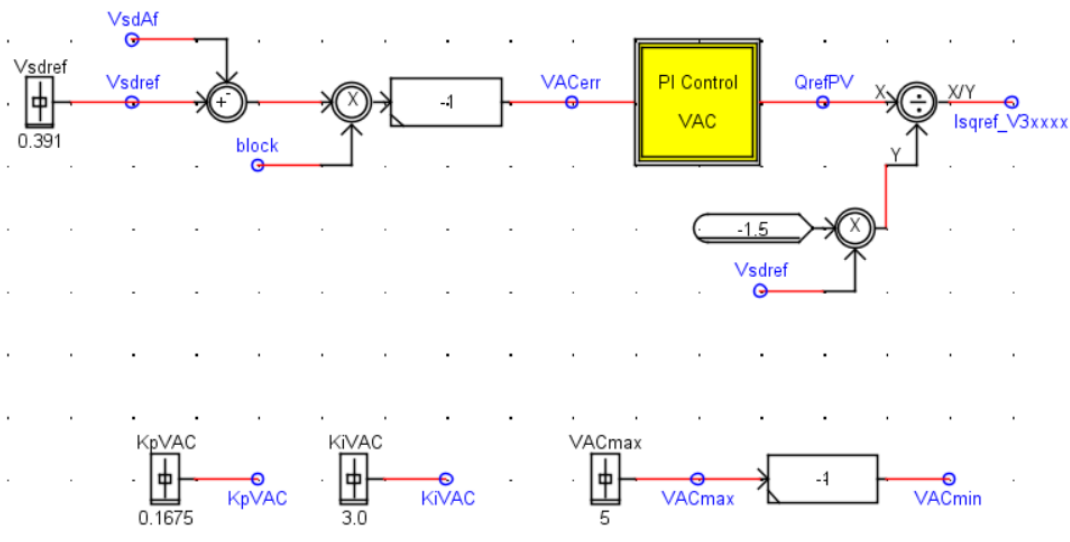


Figure C.9: Voltage control during transition



# Bibliography

- [1] C. Muller, S. Raths, S. Koopmann, and A. Schnettler, "Analysis of alternative transition paths for the German energy system," in Proceedings - 2016 51st International Universities Power Engineering Conference, UPEC 2016, 2017.
- [2] A. G. Boulanger, A. C. Chu, S. Maxx, and D. L. Waltz, "Vehicle electrification: Status and issues," in Proceedings of the IEEE, 2011.
- [3] P. Capros et al., "Outlook of the EU energy system up to 2050: The case of scenarios prepared for European Commission's 'clean energy for all Europeans' package using the PRIMES model," Energy Strateg. Rev., 2018.
- [4] A. S. Chuang and C. Schwaegerl, "Ancillary Services for Renewable Integration."
- [5] M. Brenna, F. Foiadelli, M. Longo, and D. Zaninelli, "Ancillary services provided by BESS in a scenario characterized by an increasing penetration of unpredictable renewables," in 2017 IEEE PES Innovative Smart Grid Technologies Conference Europe, ISGT-Europe 2017 - Proceedings, 2018.
- [6] Z. Mehdi, M. Esmail, H. Golshan, and J. M. Guerrero, "Distributed Control of Battery Energy Storage Systems for Voltage Regulation in Distribution Networks With High PV Penetration," IEEE Trans. Smart Grid, vol. 9, no. 4, 2018.
- [7] D. Zhu and Y. J. A. Zhang, "Optimal coordinated control of multiple battery energy storage systems for primary frequency regulation," IEEE Trans. Power Syst., 2019.
- [8] Y. Malachi and S. Singer, "A genetic algorithm for the corrective control of voltage and reactive power," IEEE Trans. Power Syst., 2006.
- [9] A. Gandhi, "Reactive Power Sharing Control Strategy Based on Droop Control in Islanded Microgrid," no. July, pp. 160–163, 2016.
- [10] Y. Chen, J. Zhao, J. Wang, K. Qu, S. Ushiki, and M. Ohshima, "A Decoupled PQ Control strategy of Voltage- Controlled Inverters," pp. 1374–1379, 2015.
- [11] R. Sebastián, "Application of a battery energy storage for frequency regulation and peak shaving in a wind diesel power system," IET Gener. Transm. Distrib., 2016.
- [12] I. Serban and C. Marinescu, "An enhanced three-phase battery energy storage system for frequency control in microgrids," in Proceedings of the International Conference on Optimisation of Electrical and Electronic Equipment, OPTIM, 2012.
- [13] M. Khalid and A. Savkin, "Model predictive control based efficient operation of battery energy storage system for primary frequency control," Control Autom. Robot. Vis. (ICARCV), 2010 11th Int. Conf., pp. 2248–2252, 2010.
- [14] T. R. Ayodele and A. S. O. Ogunjuyigbe, "Mitigation of wind power intermittency: Storage technology approach," Renew. Sustain. Energy Rev., vol. 44, pp. 447–456, 2015.
- [15] M. Durrant, H. Werner, and K. Abbott, "Model of a VSC HVDC terminal attached to a weak AC system," in Proceedings of 2003 IEEE Conference on Control Applications, 2003. CCA 2003.
- [16] V. Soares, P. Verdelho, and G. D. Marques, "An instantaneous active and reactive current component method for active filters," IEEE Trans. Power Electron., 2000.

- [17] L. Wu, H. Liu, K. Bai, and Z. Cui, "A coordinated control strategy of active power and voltage for large scale wind-storage combined generation system," C. 2016 - Int. Conf. Cond. Monit. Diagnosis, pp. 811–814, 2016.
- [18] T. Morstyn, B. Hredzak, and V. G. Agelidis, "Control Strategies for Microgrids with Distributed Energy Storage Systems: An Overview," *IEEE Trans. Smart Grid*, vol. 9, no. 4, pp. 1–1, 2016.
- [19] A. S. Chandran and P. Lenin, "A review on active & reactive power control strategy for a standalone hybrid renewable energy system based on droop control," in 2018 International Conference on Power, Signals, Control and Computation (EPSCICON), 2018.
- [20] M. Farrokhhabadi, C. A. Canizares, and K. Bhattacharya, "Evaluation of droop-based controls in an islanded microgrid with electronically interfaced distributed energy resources," in 2015 IEEE Eindhoven PowerTech, PowerTech 2015, 2015.
- [21] B. Wei, J. M. Guerrero, J. C. Vasquez, and Xiaoqiang Guo, "A modified droop control method for parallel-connected current source inverters," in IECON 2016 - 42nd Annual Conference of the IEEE Industrial Electronics Society, 2016.
- [22] S. Teleke, M. E. Baran, S. Bhattacharya, and A. Q. Huang, "Rule-based control of battery energy storage for dispatching intermittent renewable sources," *IEEE Trans. Sustain. Energy*, vol. 1, no. 3, pp. 117–124, 2010.
- [23] Q. Jiang, Y. Gong, and H. Wang, "A battery energy storage system dual-layer control strategy for mitigating wind farm fluctuations," *IEEE Trans. Power Syst.*, vol. 28, no. 3, pp. 3263–3273, 2013.
- [24] S. Faias, P. Santos, F. Matos, J. Sousa, and R. Castro, "Evaluation of energy storage devices for renewable energies integration: Application to a Portuguese wind farm," 2008 5th Int. Conf. Eur. Electr. Mark. EEM, pp. 1–7, 2008.
- [25] S. W. Mohod and M. V. Aware, "Energy storage to stabilize the weak wind generating grid," 2008 Jt. Int. Conf. Power Syst. Technol. POWERCON IEEE Power India Conf. POWERCON 2008, 2008.
- [26] T. Tanabe, T. Sato, R. Tanikawa, I. Aoki, T. Funabashi, and R. Yokoyama, "Generation scheduling for wind power generation by storage battery system and meteorological forecast," *IEEE Power Energy Soc. 2008 Gen. Meet. Convers. Deliv. Electr. Energy 21st Century, PES*, pp. 1–7, 2008.
- [27] Y. Wen, C. Guo, D. S. Kirschen, and S. Dong, "Enhanced security-constrained OPF with distributed battery energy storage," *IEEE Trans. Power Syst.*, vol. 30, no. 1, pp. 98–108, 2015.
- [28] F. Palone et al., "Commissioning and testing of the first Lithium-Titanate BESS for the Italian transmission grid," 2015 IEEE 15th Int. Conf. Environ. Electr. Eng. EEEIC 2015 - Conf. Proc., pp. 1025–1030, 2015.
- [29] J. A. Mundackal, A. C. Varghese, P. Sreekala, and V. Reshmi, "Grid power quality improvement and battery energy storage in wind energy systems," 2013 Annu. Int. Conf. Emerg. Res. Areas, AICERA 2013 2013 Int. Conf. Microelectron. Commun. Renew. Energy, ICMiCR 2013 - Proc., pp. 1–6, 2013.
- [30] L. Xiacong, K. Lingyi, L. Liying, L. Bo, and W. Zhongyong, "Improvement of power quality and voltage stability of load by battery energy storage system," *POWERENG 2009 - 2nd Int. Conf. Power Eng. Energy Electr. Drives Proc.*, pp. 227–232, 2009.
- [31] D. Sutanto, "Power management solutions for energy management, power quality and environment using battery energy storage systems," no. July, p. 15 vol.1, 2008.

- [32] T. Yunusov, D. Frame, W. Holderbaum, and B. Potter, "The impact of location and type on the performance of low-voltage network connected battery energy storage systems," *Appl. Energy*, vol. 165, pp. 202–213, 2016.
- [33] L. Mardira, T. K. Saha, and M. Eghbal, "Investigating impacts of battery energy storage systems on electricity demand profile," 2014 Australas. Univ. Power Eng. Conf. AUPEC 2014 - Proc., no. October, pp. 1–5, 2014.
- [34] M. S. Whittingham, "History, evolution, and future status of energy storage," *Proc. IEEE*, vol. 100, no. SPL CONTENT, pp. 1518–1534, 2012.
- [35] J. M. Guerrero, L. Hang, and J. Uceda, "Control of distributed uninterruptible power supply systems," *IEEE Trans. Ind. Electron.*, 2008.
- [36] M. H. Weik, "Management Network," *Comput. Sci. Commun. Dict.*, vol. 51, no. 6, pp. 971–971, 2006.
- [37] Y. Simmhan, A. G. Kumbhare, B. Cao, and V. Prasanna, "An analysis of security and privacy issues in smart grid software architectures on clouds," *Proc. - 2011 IEEE 4th Int. Conf. Cloud Comput. CLOUD 2011*, pp. 582–589, 2011.
- [38] G. C. Lazaroiu, V. Dumbrava, S. Leva, M. Roscia, and M. Teliceanu, "Virtual power plant with energy storage optimized in an electricity market approach," 5th Int. Conf. Clean Electr. Power Renew. Energy Resour. Impact, ICCEP 2015, pp. 333–338, 2015.
- [39] P. Mercier, R. Cherkaoui, and A. Oudalov, "Optimizing a battery energy storage system for frequency control application in an isolated power system," *IEEE Trans. Power Syst.*, 2009.
- [40] A. Oudalov, D. Chartouni, and C. Ohler, "Optimizing a battery energy storage system for primary frequency control," *IEEE Trans. Power Syst.*, 2007.
- [41] M. Swierczynski, D. Loan Stroe, A. I. Stan, and R. Teodorescu, Primary Frequency Regulation with Li-ion Battery Energy Storage System: a Case Study for Denmark. .
- [42] D. Zhu and Y. J. A. Zhang, "Optimal coordinated control of multiple battery energy storage systems for primary frequency regulation," *IEEE Trans. Power Syst.*, 2019.
- [43] L. Wu, H. Liu, K. Bai, and Z. Cui, "A coordinated control strategy of active power and voltage for large scale wind-storage combined generation system," C. 2016 - Int. Conf. Cond. Monit. Diagnosis, pp. 811–814, 2016.
- [44] C. K. Zhang, L. Jiang, Q. H. Wu, Y. He, and M. Wu, "Delay-dependent robust load frequency control for time delay power systems," *IEEE Trans. Power Syst.*, 2013.
- [45] L. Cheng, G. Chen, W. Gao, F. Zhang, and G. Li, "Adaptive time delay compensator (ATDC) design for wide-area power system stabilizer," *IEEE Trans. Smart Grid*, 2014.
- [46] J. W. Stahlhut, T. J. Browne, G. T. Heydt, and V. Vittal, "Latency viewed as a stochastic process and its impact on wide area power system control signals," *IEEE Trans. Power Syst.*, 2008.
- [47] A. V. Nedolivko and A. N. Belyaev, "Improvement of transient stability analysis methods in verification of wide area control systems for long-distance AC interconnection," in *Proceedings of the 2016 IEEE North West Russia Section Young Researchers in Electrical and Electronic Engineering Conference, EIconRusNW 2016*, 2016.
- [48] M. Ndreko, "Offshore Wind Plants with VSC-HVDC Connection and their Impact on the Power System Stability: Modeling and Grid Code Compliance."
- [49] N. Mohan, T. M. Undeland, and W. P. Robbins, *Switch-mode dc-ac inverters: dc - sinusoidal ac*. 2003.

- 
- [50] A. De, V. Jaén, E. Acha, S. Member, and A. G. Expósito, “Voltage Source Converter Modeling for Power System State Estimation : STATCOM and VSC-HVDC,” vol. 23, no. 4, pp. 1552–1559, 2008.
- [51] M. L. Remus Teodorescu and P. Rodriguez, “Grid Converters for Photovoltaic and Photovoltaic and,” pp. 51–56, 2011.
- [52] K. Strunz, Benchmark Systems for Network Integration of Renewable and Distributed Energy Resources Task Force C6.04 Benchmark Systems for Network Integration of Renewable and Distributed Energy Resources. 2014.
- [53] M. Chen, S. Member, and G. A. Rinc, “Accurate Electrical Battery Model Capable of Predicting Runtime and I – V Performance,” vol. 21, no. 2, pp. 504–511, 2006.